



Landsvirkjun

LV-2019-061

VATNAJÖKULL:

Mass balance, meltwater drainage and
surface velocity of the glacial year
2017-18

Lykilsíða



Skýrsla LV nr: LV-2019-061

Dags: 25.09.2019

Fjöldi síðna: 48

Upplag: 1

Dreifing:

- Birt á vef LV
- Opin
- Takmörkuð til

Titill: VATNAJÖKULL: Mass balance, meltwater drainage and surface velocity of the glacial year 2017-18

Höfundar/fyrirtæki: Finnur Pálsson, Jarðvísindastofnun Háskóla Íslands

Verkefnisstjóri: Andri Gunnarsson

Unnið fyrir: Landsvirkjun

Samvinnuaðilar: Jarðvísindastofnun Íslands

Útdráttur: For the glaciological year 2017-18 winter balance for Vatnajökull exceeded the average, over the observation period from 1991-92, by ~10%. The total summer mass loss was about 80% of the average since 1995. The net balance was negative as it has been since 1994-95 (except 2014-15), but now only marginally so, just as last year 2016-17. The about 20 year period of high mass loss seems to have halted; the past few years have all had net balance close to zero, and there has been a positive trend in the net balance since about 2009, although with high variability. The 2017-18 close to zero balance is primarily explained by summer mass loss less than the average of the survey period.

Lykilorð: Jöklar, afkoma, Vatnajökull

ISBN nr:

Samþykki verkefnisstjóra
Landsvirkjunar

A handwritten signature in blue ink that reads 'Andri Gunnarsson'.

VATNAJÖKULL

Mass balance, meltwater drainage and
surface velocity of the glacial year
2017-18

Contents:

1. Introduction	2
2. Diary	2
3. Mass balance measurements	3
3.1 Methods	3
3.2 Results of mass balance measurements	4
3.2.1. Tungnaárjökull	9
3.2.2. Köldukvíslarjökull	9
3.2.3. Dyngjujökull	10
3.2.4. Brúarjökull	11
3.2.5. Eyjabakkajökull	12
3.2.6. Breiðamerkurjökull	12
3.2.7. Síðujökull	13
3.2.8. Grímsvötn	14
3.3. The mass balance record for Vatnajökull	14
4. Surface velocity measurements	17
5. Melt water runoff	18
6. Conclusions	20
Figures:	
Figure 1. Outlets of Vatnajökull and location of mass balance sites in 2017_18.	4
Figure 2. Maps showing point values of specific in m water equivalent (m_{we}), 2017_18.	5
Figure 3. a. Specific mass balance (m_{we}), along all mass balance profiles 2017_18. b. Specific mass balance as a function of elevation on central flow lines on Vatnajökull outlets.	6
Figure 4. Specific mass balance of Vatnajökull (m_{we}) 2017_18. Top: winter, Centre: summer Bottom: net balance.	7
Figure 5. Top left: The difference between winter balance in 2017_18 and the average winter balance 1995_96 to 2016_17. Top right: The difference between summer balance in 2018 and the average summer balance 1996 to 2017. Lower left: The difference between net balance in 2017_18 and the average net balance 1995_96 to 2016_17.	8
Figure 6. Mass balance at a central flow line on Tungnaárjökull 2017_18, and average mass balance 1991_92 to 2016_17.	9
Figure 7. Specific mass balance at a central flow line on Köldukvíslarjökull 2017_18, and average mass balance 1991_92 to 2016_17.	9
Figure 8. Mass balance at a central flow line on Dyngjujökull 2017_18, and average mass balance 1992_93 to 2016_17.	10
Figure 9. Mass balance at two flow lines on Brúarjökull 2017_18, and average mass balance 1992_93 to 2016_17.	11
Figure 10. Mass balance at a central flow line on Eyjabakkajökull 2017_18, and average mass balance 1995_96 to 2015_16.	12
Figure 11. Mass balance at a central flow line on Breiðamerkurjökull 2017_18, and average mass balance 1995_96 to 2016_17.	12
Figure 12. Mass balance at a central flow line on Síðujökull 2017_18, and average mass balance 2004_05 to 2016_17.	13
Figure 13. Mass balance at a central flow line towards Grímsvötn 2017_18, and average mass balance 1991_92 to 2016_17.	13
Figure 14. Specific mass balance record of Vatnajökull 1991_92 – 2017_18.	14
Figure 15. Cumulative specific mass balance of Vatnajökull 1991_92 – 2017_18.	14
Figure 16. Specific mass balance for Vatnajökull outlets 1991_92 – 2017_18.	15
Figure 17. Cumulative specific mass balance of Vatnajökull outlets 1991_92 – 2017_18.	16
Figure 18. The relation between net annual balance (b_n) and accumulation area ratio (AAR) and b_n and equilibrium line altitude (ELA), for Vatnajökull outlets during the survey period.	16
Figure 19. Average surface velocity at survey sites in 2017_18.	17
Figure 20. Water divides and drainage basins of selected rivers draining water from Vatnajökull.	18
Figure 21. The temporal variation of the average annual meltwater runoff to selected river catchments.	18
Tables:	
Table I. Melt water drainage to selected rivers.	19
Appendixes:	
Appendix A: Mass balance at survey sites 2017_18.	21
Appendix B: Balance distribution by elevation in 2017_18.	23
Appendix C: Coordinates at velocity measurement sites, and overview of surface elevation profiles.	31
Appendix D: Measured surface velocity on Vatnajökull in 2017_18.	35
Appendix E: Melt water runoff to selected rivers in summer 2018 derived from summer ablation.	37
Appendix F: location of GPS surface profiles 2018.	48

1. INTRODUCTION

In 1992 (glacial year 1991_92) a program of mass balance measurements was started for Vatnajökull by the Science Institute University of Iceland (now Institute of Earth Sciences, IES) in collaboration with the National Power Company (NPC). For the first year the program was limited to the western part of the glacier, but then expanded to include the northern outlets as well. In 1996 this study was further expanded to include southern outlets, with support from The European Union (Framework IV - Environment and Climate, TEMBA project 1996-1997). This program was extended 1998–2000 with further support from EU (Framework IV - Environment and Climate, ICEMASS project, 1998-2000). In 2000-2002 NPC and IES continued the program. In 2003-2005 IES participated in a multinational research project, which was financially supported by The European Union (EVK2-CT-2002-00152 SPICE). IES was responsible for obtaining data sets for calibration of models of the mass balance and dynamics of Vatnajökull. This work was also supported by The National Power Company of Iceland and The National Road Authority, and was a continuation of the TEMBA-project of 1996-97 and ICEMASS project 1998-2001.

In since then IES and NPC have continued a similar program. Mass balance measurements on the southeast outlets Breiðamerkurjökull and Hoffellsjökull is financially supported by the National Road Authority.

The aim of the collaborative work of NPC and IES is to improve our understanding of the mass balance and melt water runoff from glaciers. This work in combination with energy balance measurements by NPC and IES on Vatnajökull will be used for calibration of models of the energy and mass balance of Vatnajökull.

This report describes the field measurements, mass balance, melt water runoff and GPS survey, for the glacial year 2017_18.

2. DIARY

Mars 23 - 24: installation of melt wires, maintenance of AWSs on Breiðamerkurjökull

May 8 - 14: measurements of the winter balance, setup of AWSs.

June 2-8: measurements of the winter balance, setup of AWS on Bárðarbunga.

October 8 – 12: summer balance measurements, take down of AWSs, maintenance of AWSs on Breiðamerkurjökull.

In all expeditions and short visits to the glacier the locations of mass balance stakes were measured with Kinematic GPS (or fast static GPS) for surface velocity calculation.

The following members of staff of the Institute of Earth Sciences, University of Iceland, carried out the fieldwork on Vatnajökull: Finnur Pálsson, Sveinbjörn Steinþórsson, Eyjólfur Magnússon with Andri Gunnarsson, Gestur Jónsson and (National Power Company) and Hlynur Skagfjörð Pálsson and Karl Eiríksson (Reykjavík Rescue Team).

Members of the Iceland Glaciological Society and staff of Iceland Meteorological office participated in the June fieldwork.

3. MASS BALANCE MEASUREMENTS

The purpose of the mass balance measurements is to describe the temporal and spatial distribution of the components of the mass balance. The mean annual values of the components and their variation from year to year are analyzed and related to meteorological conditions and climatic variability. The results will be used in studies of changes in the glacier volume, estimates of meltwater contribution to glacial rivers, mass balance modeling, evaluation of altitudinal and regional variations of mass balance in response to climatic variations, and to assess the hydrometeorological and dynamic response of the ice cap to climate change.

The mass balance was determined by a stratigraphic method, measuring changes in thickness and density relative to the summer surface. The winter balance was estimated by drilling ice cores through the winter layer in the spring. Ablation was monitored from markers; snow stakes were put up on the glacier and wires were drilled down in the ablation area. The summer balance was measured in the autumn.

3.1 Methods

Measurements of the surface mass balance on a large ice cap like Vatnajökull are impractical in terms of cost with conventional techniques and sampling density that are typically used on small glaciers. The spatial variability of the mass balance may, however, be predictable on the flat large outlets of such an ice cap given data on several profiles extending over the elevation range of the glacier. The precipitation generally increases with elevation and decreases with the distance from the coast, but both the distribution of snowfall and

redistribution of snow by drift depend on the prevailing wind direction during the winter. The summer melting depends mainly on the altitude and the albedo of the glacier surface. Therefore, we have used observations along a limited number of flowlines, which span the elevation range of the outlets to assess aerial estimates of surface mass balance. Each profile describes the variation with elevation, but together they also describe the lateral variation of the mass balance. Recently, modern over-snow vehicles and helicopters have allowed fast traverses to ensure successful fieldwork in spite of frequently poor weather conditions. The error for individual point measurement is estimate $\sim 30 \text{ cm}_{\text{we}}$ for both summer and winter balance. The error for the area integral of mass balance is however considered smaller, since the error for individual survey sites is independent.

The winter mass balance (b_w) is defined as the mass of snow accumulated during the winter months, the summer balance (b_s) is the mass balance during the summer, and the net balance (b_n) is defined as their sum. The specific mass balance is expressed in terms of the equivalent thickness of water. All mass balance components apply to a time interval between given measurement dates, which are not fixed from one year to another. The dates in the autumn are separated by approximately one calendar year, which roughly coincides with the glaciological year defined as October 1st to September 30th. Snow cores are drilled in April-May through the winter layer and profiles of the density are measured. The summer balance is derived in the autumn from measurements of the changes in the snow core density during the summer in the accumulation area and from readings at stakes and wires drilled into the ice in the ablation areas.

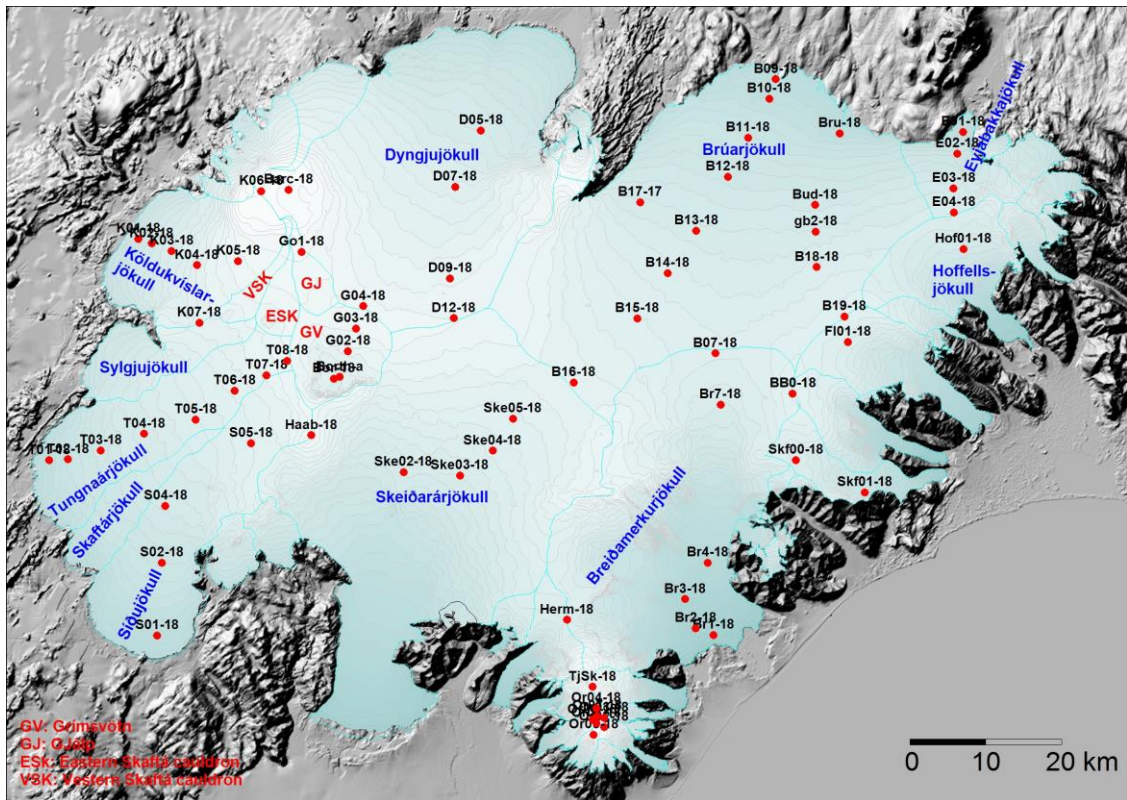


Figure 1. Outlets of Vatnajökull and location of mass balance survey sites 2017_18.

Digital maps are created for winter, summer and net balance for the whole ice cap based on site measurements. The mass balance is calculated over both the ice and water drainage basins. The summer balance over the water basin is an estimate of meltwater contribution to rivers and groundwater storage. This estimate, however, does not include precipitation that falls as rain on the glacier or snow, which falls and melts during the summer. The meltwater contribution is compared with river runoff at stream flow gauges closest to the glacier. For this comparison, we define the glaciological year from the start of October to the end of September and the period draining meltwater from the glacier during the summer from June through September. It would be misleading to include May in the summer period because runoff from the glacier melt in May is delayed due to refreezing during elimination of the cold wave.

3. 2 Results of mass balance measurements.

Mass balance measurements were done at 74 sites in spring 2018 (Fig. 1). The specific mass balance at individual sites is shown in Fig. 2. Most sites are on central flow lines at individual outlets. The specific mass balance along approximate flow lines is given in Fig 3. for the glacier outlets: Síðujökull, Tungnaárjökull, Köldukvíslarjökull, Dyngjujökull, Brúarjökull (west and east), Eyjabakkajökull, Hoffellsjökull and Breiðamerkurjökull.

Digital maps for winter, summer and net balance are shown in Figure 4. Although no balance measurements are available for Skeiðarárjökull, the balance has been estimated by interpolating the balance values from the neighboring outlets, based on our experience from previous years. The mass balance of individual outlet is discussed in the following subsections.

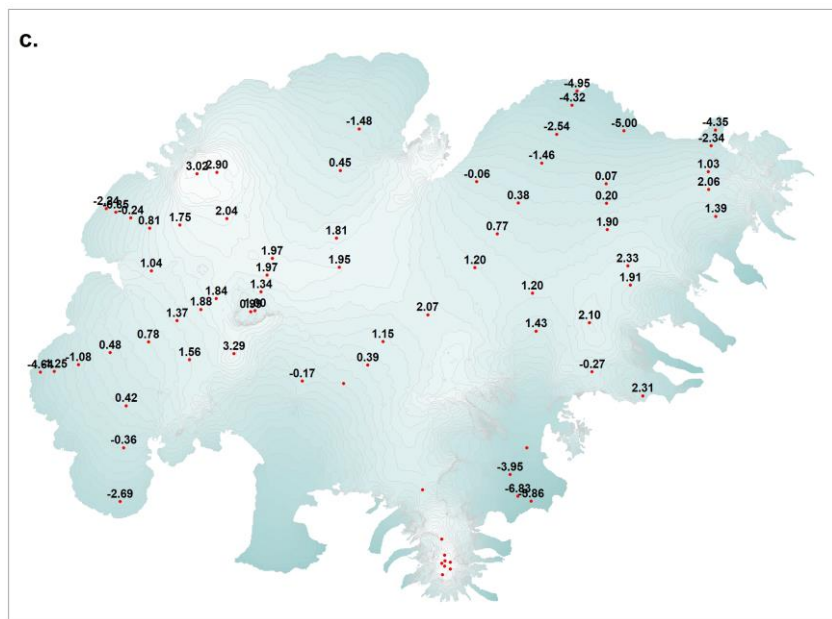
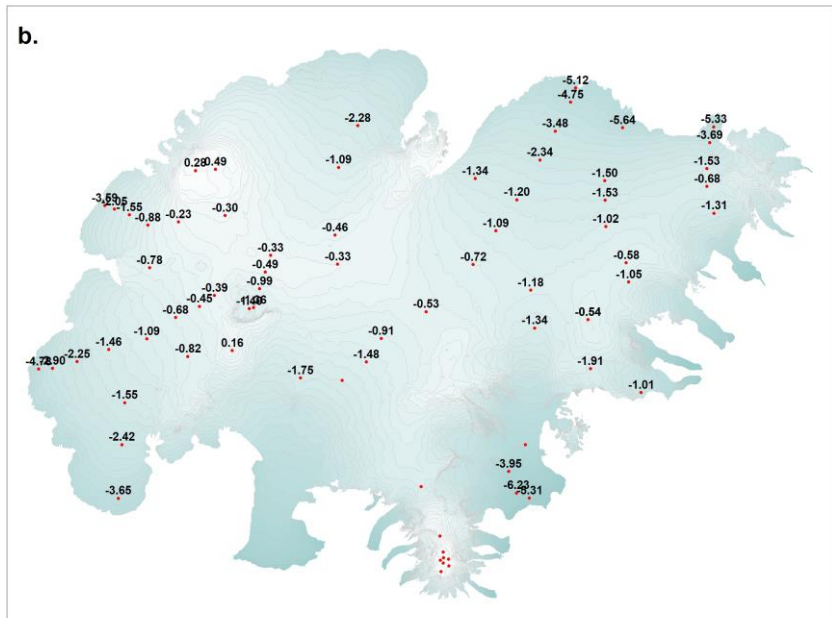
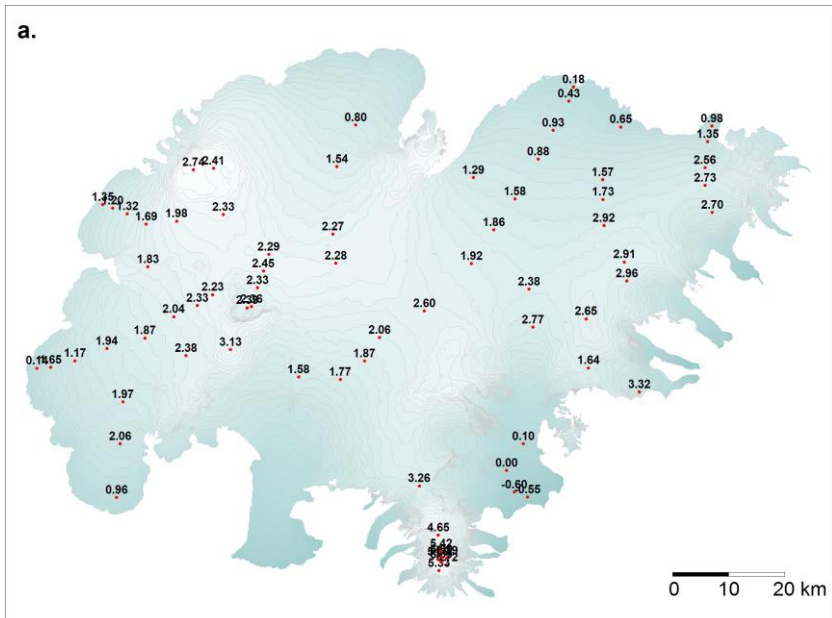


Figure 2. Maps showing point values of specific mass balance in m water equivalent (m_{we}), 2017_18. a. winter, b. summer, c. net balance.

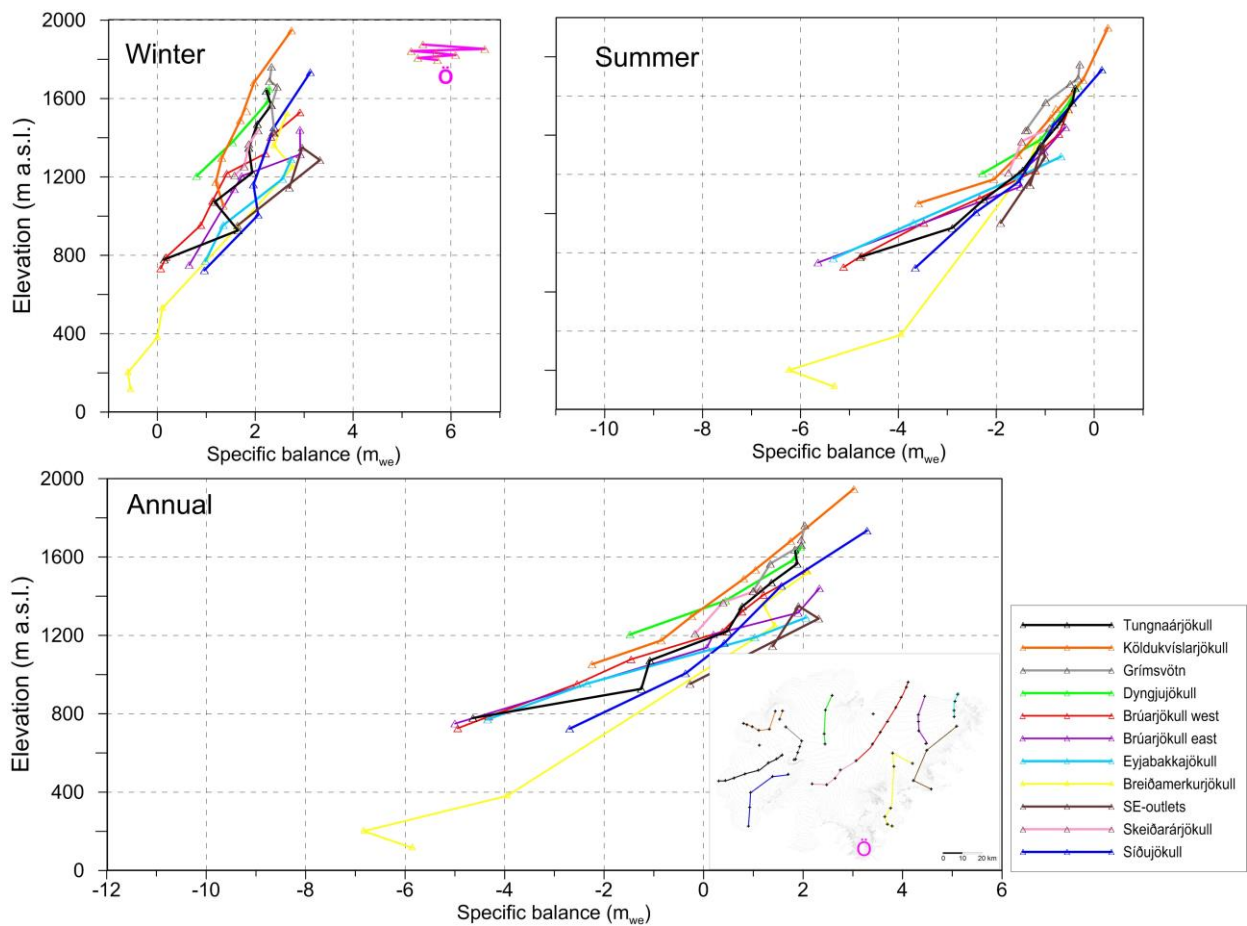


Figure 3. a. Specific mass balance (m_{we}), along all mass balance profiles 2017_18.

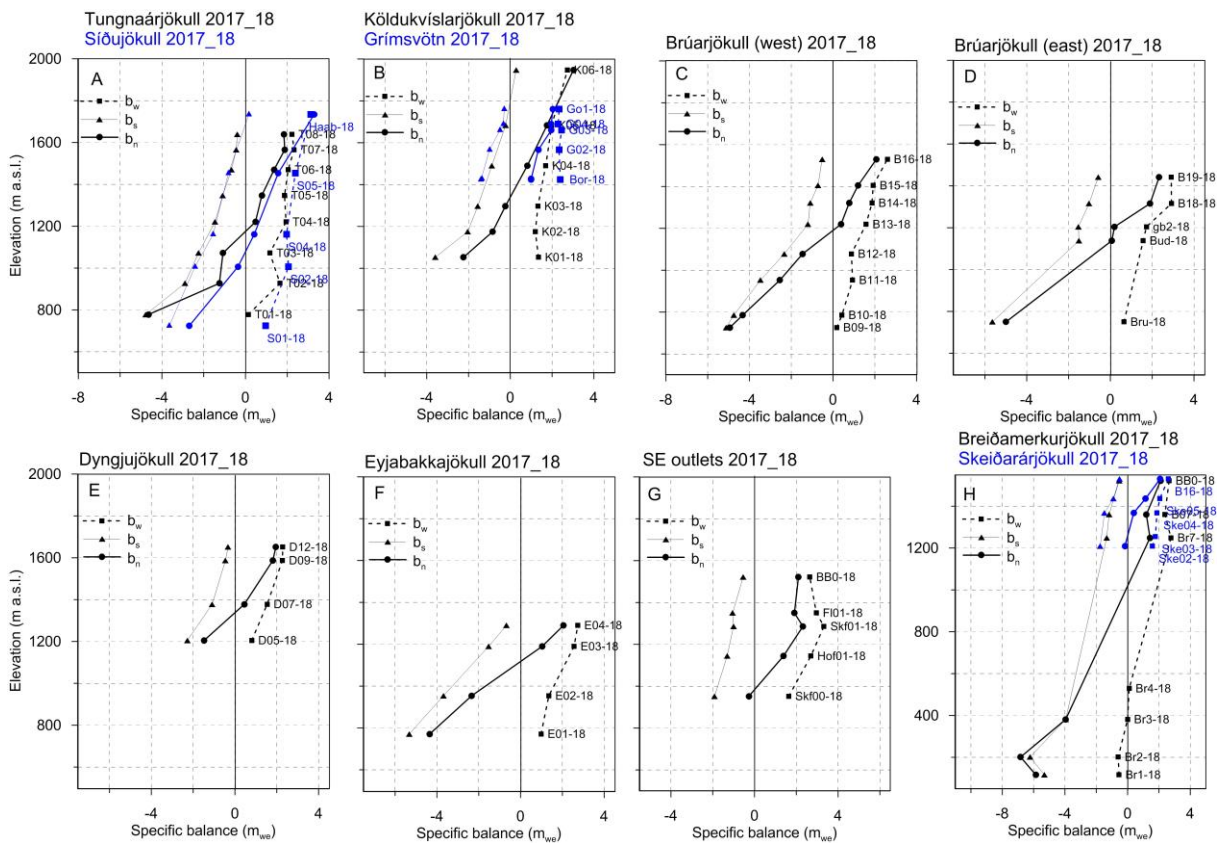


Figure 3. b. Specific mass balance (m_{we}) 2017_18 as a function of elevation on central flow lines on Vatnajökull outlets.

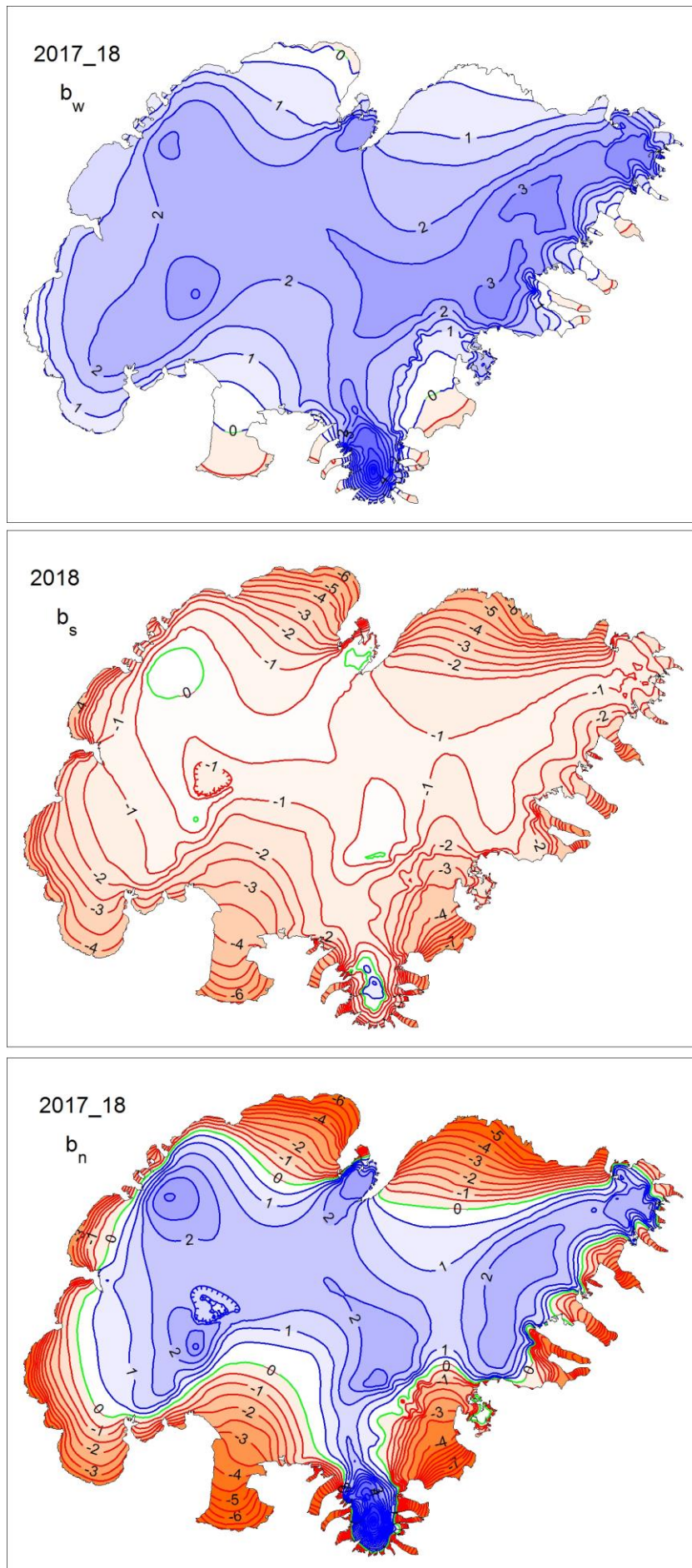


Figure 4. Specific mass balance (m_{we}) maps of Vatnajökull 2017_18. Top: winter, Centre: summer, Bottom: net balance.

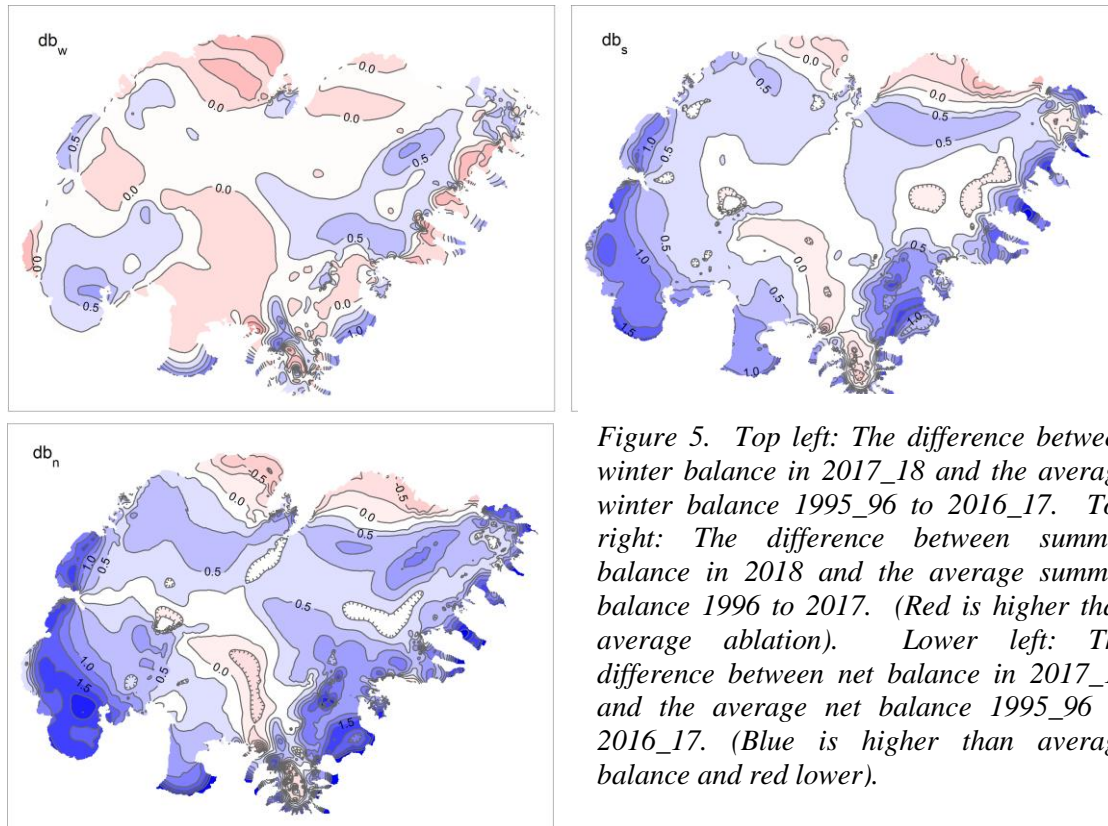


Figure 5. Top left: The difference between winter balance in 2017_18 and the average winter balance 1995_96 to 2016_17. Top right: The difference between summer balance in 2018 and the average summer balance 1996 to 2017. (Red is higher than average ablation). Lower left: The difference between net balance in 2017_18 and the average net balance 1995_96 to 2016_17. (Blue is higher than average balance and red lower).

A surface DEM is needed for surface area distribution and delineation of ice divides for individual outlets and catchments. The current DEM is mostly based on SPOT5 satellite images in 2010, and partly from LiDAR survey 2010, -11 and -12 (Jóhannesson et al. 2013), but the large set of GPS profile measured in spring 2015 was used to locally shift the older DEMs. This new DEM representing the surface of 2015 was used in all area distributions, but ice and water divides were not reworked.

The weather in the autumn and first winter months, 2017-18, was wet but and rather warm, not much snow below ~1000 m. The latter half winter into, especially February and May were also relatively warm with more than average precipitation. The spring was relatively cold and dry.

Figure 5 (top left) shows that the winter accumulation is over average at all the high accumulation zone and in the SW, but less than average in the north. Winter melting at the low lying S outlets was less than average.

First summer months were cold, calm and mostly dry, but cloudy, and even wet in the S and SW over Vatnajökull. Melting at lower ablation zone extended well into October and even November. This resulted in total melt by far less than average melt in the ablation zone (except in the North) but close to average in the accumulation zone. The resulting net balance was higher than average on most of the glacier except on the lower regions of the N outlets.

SPOT 5 HRG images were made available by the French Space Agency (CNES) through the ISIS (Incentive for the Scientific use of Images from the SPOT system) program and SPOT 5 HRS digital elevation models by the Spot Image project Planet Action (www.planet-action.org) and the SPIRIT SPOT 5 stereoscopic survey of Polar Ice.

Jóhannesson, T., Björnsson, H., Magnússon, E., Guðmundsson, S., Pálsson, F., Sigurðsson, O., Thorsteinsson, T., and Berthier, E.:

Ice-volume changes, bias estimation of mass-balance measurements and changes in subglacial lakes derived by lidar mapping of the surface Icelandic glaciers, *Ann. Glaciol.*, 54, 63–74, doi:10.3189/2013AoG63A422,2013.

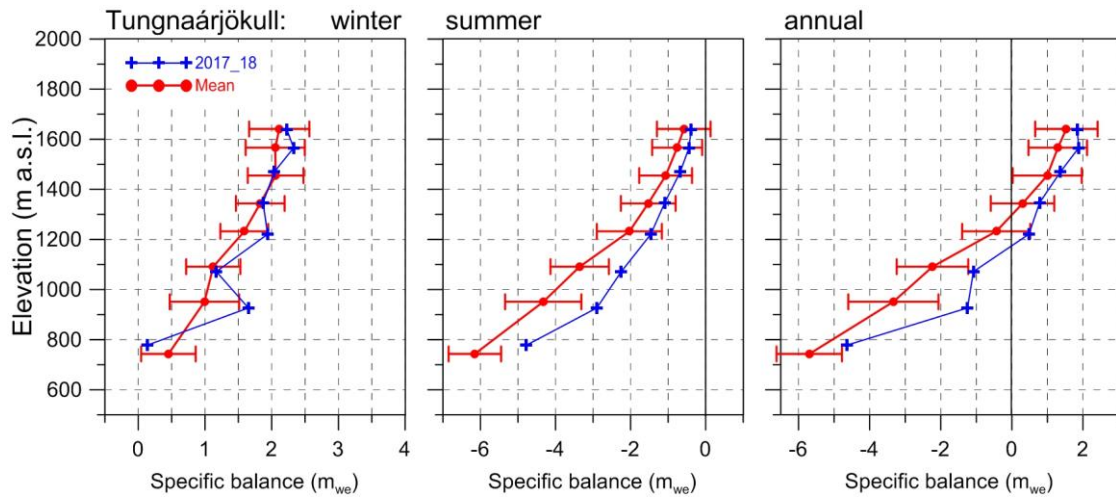


Figure 6. Mass balance at a central flow line of Tungnaárjökull 2017_18 and average mass balance 1991_92 to 2016_17.

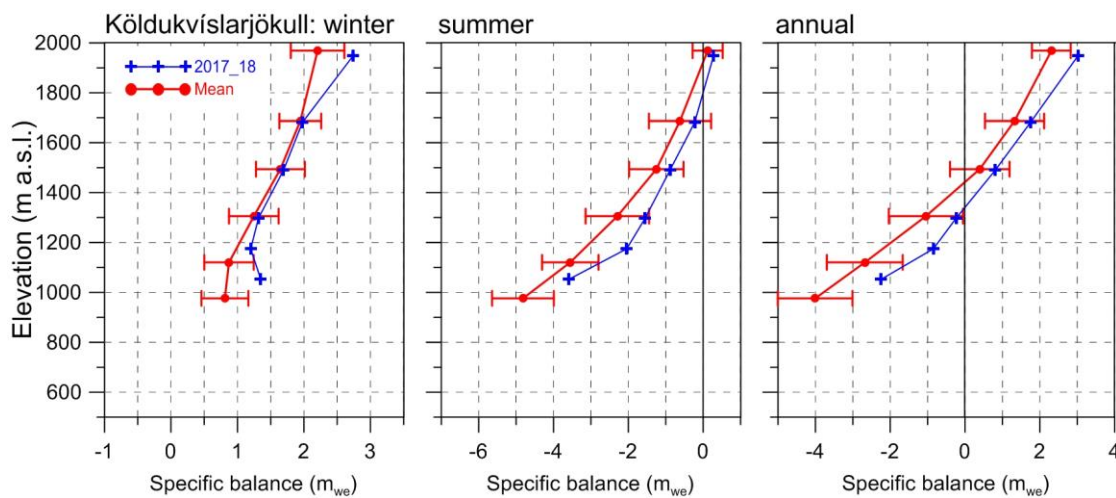


Figure 7. Mass balance at a central flow line of Köldukvíslarjökull 2017_18 and average mass balance 1991_92 to 2016_17.

3.2.1 Tungnaárjökull.

Area = 340 km²

$B_w = 0,54 \text{ km}^3_{we}$; $b_w = 1,58 \text{ m}_{we}$

$B_s = -0,65 \text{ km}^3_{we}$; $b_s = -1,90 \text{ m}_{we}$

$B_n = -0,11 \text{ km}^3_{we}$; $b_n = -0,32 \text{ m}_{we}$

ELA = 1175 m a.s.l. (at profile)

AAR = 58 %

(The terms are defined at the foot of this page)

Variation of mass balance along a central flow line on Tungnaárjökull is shown in Fig. 6. The winter accumulation far over average at highest and lowest survey sites, by ~1 std. The total winter balance was 4% over average. Summer melting was by far less than average at all survey sites, by far so at the lower. The summer balance was negative by only 73% of

the average during the survey period. The net balance was almost 1 std away from average at all sites, in total negative, but only 90% of the average of the survey period. This is the 24th year out of the 27 surveyed with negative net balance.

3.2.2 Köldukvíslarjökull

Area = 298 km²

$B_w = 0,49 \text{ km}^3_{we}$; $b_w = 1,64 \text{ m}_{we}$

$B_s = -0,39 \text{ km}^3_{we}$; $b_s = -1,32 \text{ m}_{we}$

$B_n = -0,10 \text{ km}^3_{we}$; $b_n = -0,32 \text{ m}_{we}$

ELA = 1340 m a.s.l. (at profile)

AAR = 62 %

Variation of mass balance along a central flow line on Köldukvíslarjökull is shown in Fig. 7. Accumulation was

For each ice catchment basin, B_w , B_s and B_n are water equivalent volumes of winter, summer and net balance, ELA the equilibrium line altitude, and AAR is the accumulation area ratio.

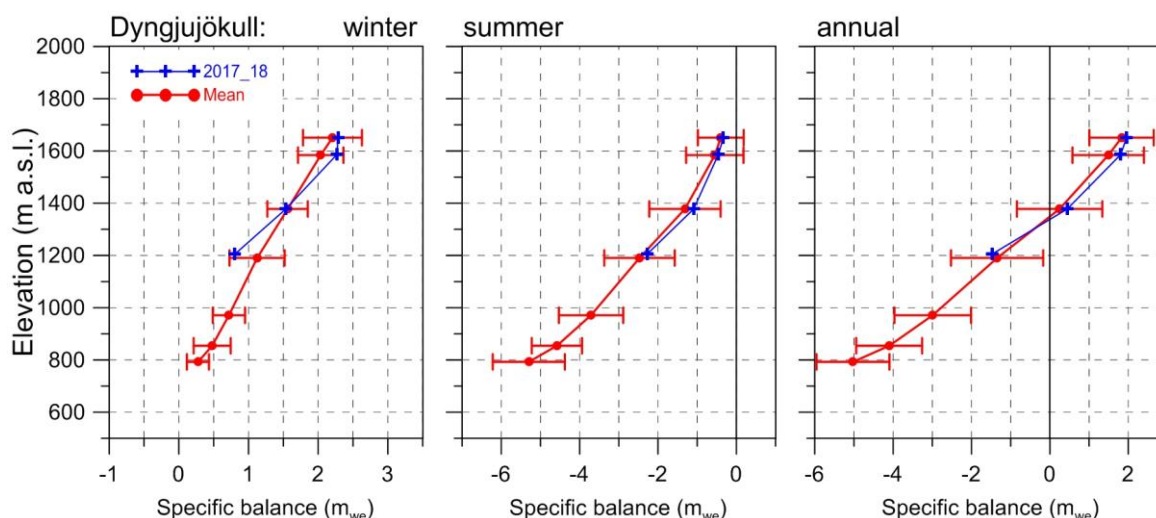


Figure 8. Mass balance at a central flow line on Dyngjufjökull 2017_18, and average mass balance 1991_92 to 2016_17 (except 1998_99 – 2003_04 at all but the top elevation).

close to average at mid elevation sites but ~ 1 std. more than average at lowest and highest sites. The total winter balance was about 11% over the average since 1991_92. Summer balance was less negative at all survey sites. In all, the summer balance was negative, by $\sim 70\%$ of the average summer of the survey period. The net balance was accordingly positive this year for the second time since 1995.

3.2.3 Dyngjufjökull

Area = 1059 km²

$B_w = 1,68 \text{ km}^3_{we}$; $b_w = 1,59 \text{ m}_{we}$

$B_s = -1,60 \text{ km}^3_{we}$; $b_s = -1,51 \text{ m}_{we}$

$B_n = 0,08 \text{ km}^3_{we}$; $b_n = 0,08 \text{ m}_{we}$

ELA = 1335 m a.s.l. (at profile)

AAR = 65 %

Variation of mass balance along a flow line on Dyngjufjökull is shown on Fig. 8. Mass balance is not measured at the lowest elevations, but assumed to be correlated (as a function of elevation) to that of Brúarjökull and Köldukvíslarjökull. Inspection of the winter Modis images suggest that at the glacier snout snow cover was very thin, less than average below 1400 m but over average in the high accumulation zone. The total winter

balance was very close to average.

Summer balance was very close to average at all survey sites. The summer balance was negative, at $\sim 95\%$ of an average summer. The net balance was slightly positive, now 0,08 m_{we} while the average is slightly negative (-0,03 m_{we}).

Dyngjufjökull has often had mass balance close to zero, and the net balance has been estimated slightly positive in at least 6 years of the two decade period of almost continuous mass loss for Vatnajökull as a whole.

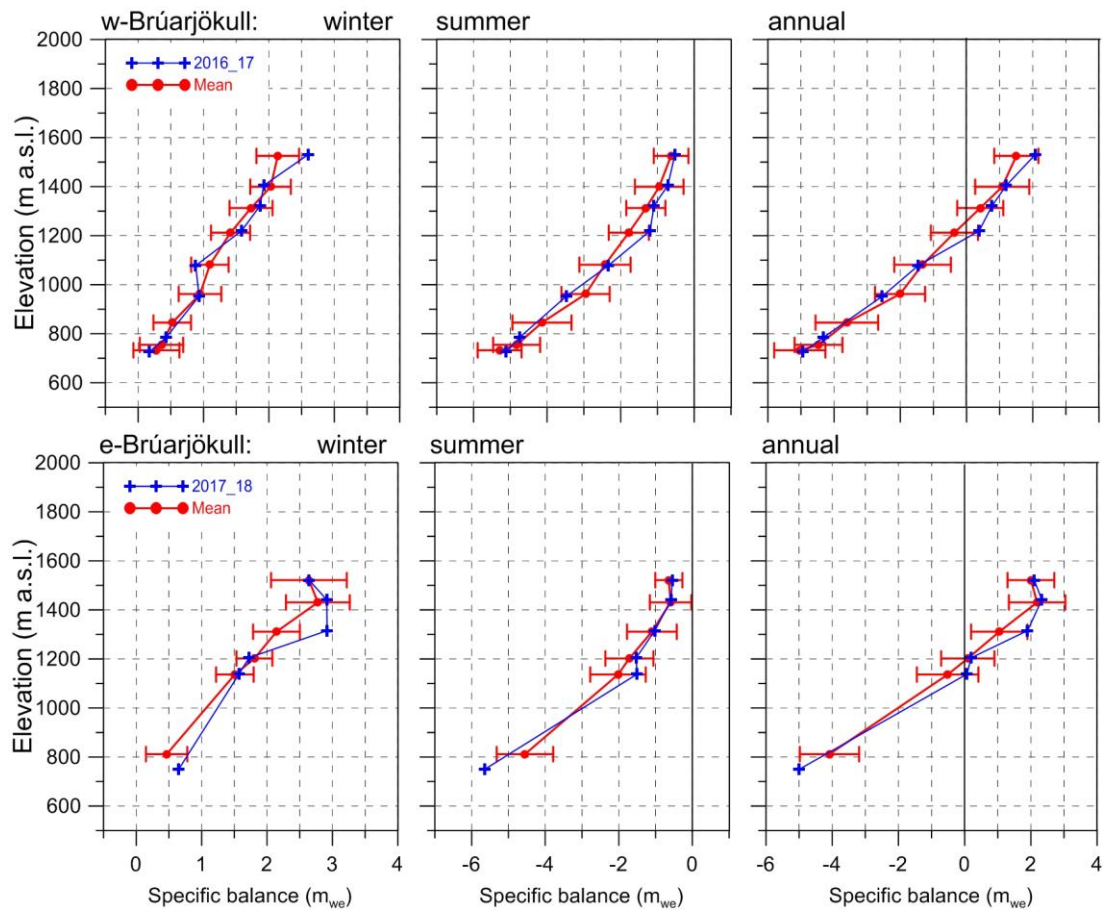


Figure 9. Mass balance at two flow lines on Brúarjökull 2017_18, and average mass balance 1992_93 to 2016_17.

3.2.4 Brúarjökull

Area = 1524 km²
 $B_w = 2,68 \text{ km}^3_{we}$; $b_w = 1,76 \text{ m}_{we}$
 $B_s = -2,59 \text{ km}^3_{we}$; $b_s = -1,70 \text{ m}_{we}$
 $B_n = 0,09 \text{ km}^3_{we}$; $b_n = 0,06 \text{ m}_{we}$
 ELA = 1190 m a.s.l. (western flow line)
 ELA = 1133 m a.s.l. (eastern flow line)
 AAR = 66 %

Variation of mass balance along two flow lines on Brúarjökull is shown on Fig. 9. Accumulation was close to average at most survey sites, not clear whether the outliers are mistakes in survey or (more likely) result from redistribution of dry snow in undulated terrain. The winter balance was about 10% higher than average since 1992_93. Summer balance (melt) was less than average in the lower accumulation zone but otherwise close

to average. The summer balance was negative by 90% of an average summer of the survey period. The net balance was close to average at most sites. In total the net balance was slightly positive (really not significantly so, in view the inherent errors of the method), but has been negative by -0.3 m_{we} on average.

During the survey period, there have been 8 years of measured positive balance and 18 years with negative.

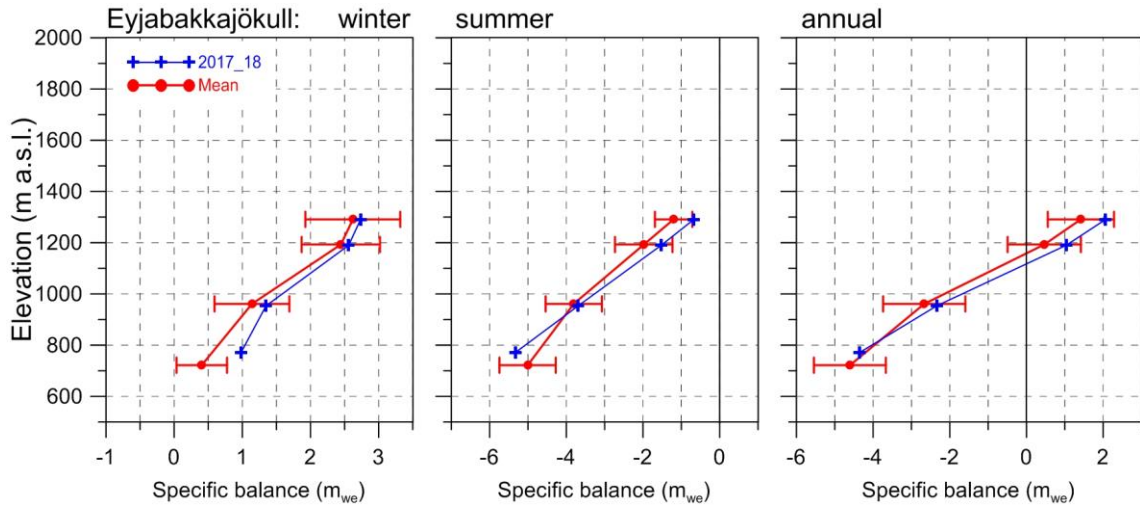


Figure 10. Mass balance at a central flow line of Eyjabakkajökull 2017_18 and average mass balance 1995_96 to 2016_17.

3.2.5 Eyjabakkajökull

Area = 112 km²

$B_w = 0,23 \text{ km}^3_{we}$; $b_w = 2,09 \text{ m}_{we}$

$B_s = -0,27 \text{ km}^3_{we}$; $b_s = -2,48 \text{ m}_{we}$

$B_n = -0,04 \text{ km}^3_{we}$; $b_n = -0,39 \text{ m}_{we}$

ELA = 1115 m a.s.l. (at profile)

AAR = 53 %

Variation of mass balance along a central flow line on Eyjabakkajökull is shown on Fig. 10. Accumulation was close average at the top sites, but up to 1 std. more than average at the lowest site reflecting cold latter half of winter. The total winter balance 2017_18 was ~15% over the average since 1995_96. Summer melting was less than average at all survey sites except the lowest, in total net loss was ~90% of average.

There was mass gain this year at the upper sites but balance close to average at the lower. In total the net balance was negative but only ~45% of the average.

3.2.6 Breiðamerkurjökull

Area = 936 km²

$B_w = 1,67 \text{ km}^3_{we}$; $b_w = 1,78 \text{ m}_{we}$

$B_s = -1,84 \text{ km}^3_{we}$; $b_s = -1,96 \text{ m}_{we}$

$B_n = -0,17 \text{ km}^3_{we}$; $b_n = -0,18 \text{ m}_{we}$

ELA = 1015 m a.s.l. (at profile)

AAR = 61 %

Variation of mass balance along a central flow line on Breiðamerkurjökull is shown on Fig. 11.

Winter accumulation was well over average at some of the survey sites in the accumulation zone, and,

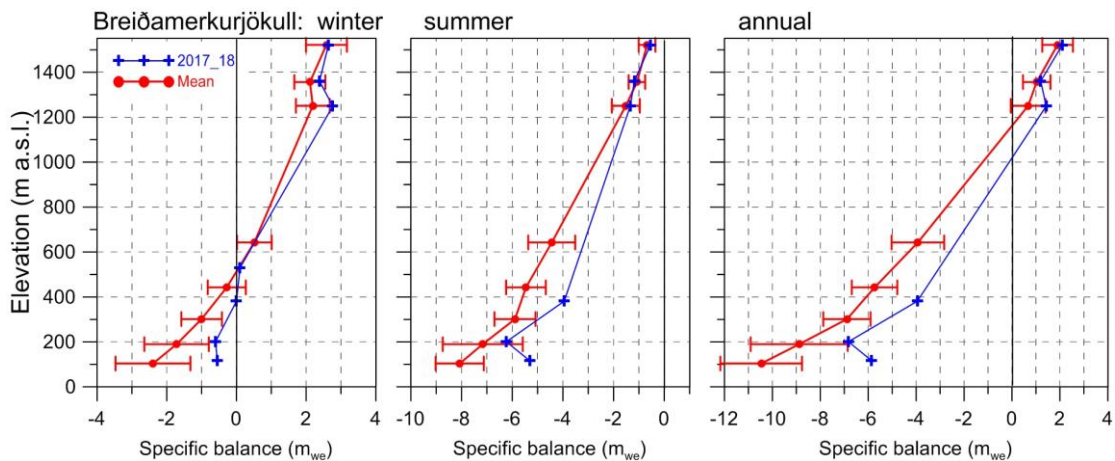


Figure 11. Mass balance at a central flow line of Breiðamerkurjökull 2017_18, and average mass balance 1995_96 to 2016_17.

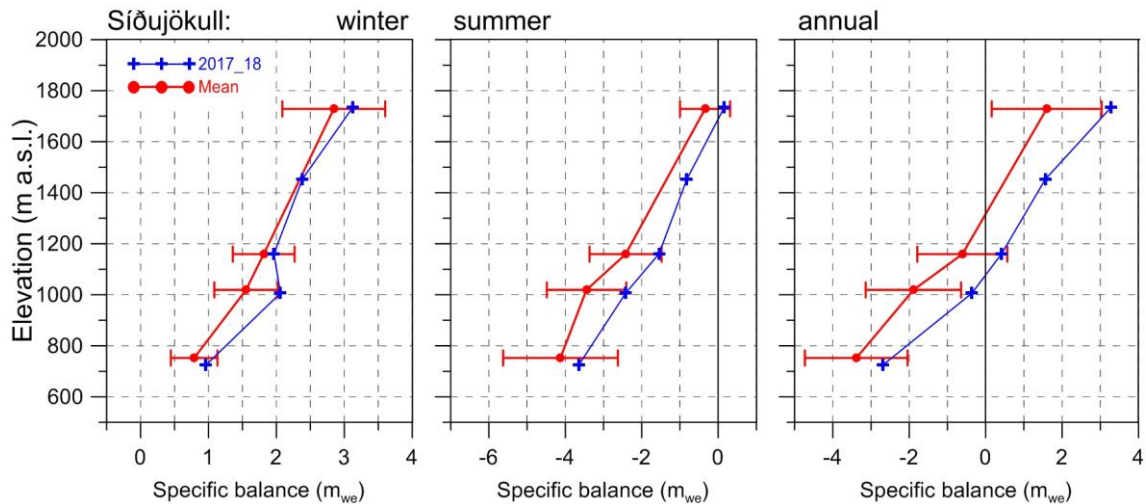


Figure 12. Mass balance at a central flow line of Síðujökull 2017_18 and average mass balance 2004_05 to 2016_17.

At the lowest sites the mass loss was about 1 std. less than average during winter. The total winter balance was ~20% over average. Summer mass loss was by far less than average at the lower sites, but close to average at the upper sites. The total summer balance mass loss was only ~75% of the average during the survey period. The net balance was negative but only by ~20% that of an average year. In addition to mass loss due to surface melt Breiðamerkurjökull loses in the order of 0,5 km³ annually via calving into the marginal lake Jökulsárlón, this is not accounted for here.

3.2.7 Síðujökull

Area = 423 km²

$B_w = 0,80 \text{ km}^3_{we}$; $b_w = 1,89 \text{ m}_{we}$

$B_s = -0,87 \text{ km}^3_{we}$; $b_s = -2,05 \text{ m}_{we}$

$B_n = -0,07 \text{ km}^3_{we}$; $b_n = -0,16 \text{ m}_{we}$

ELA = 1015 m a.s.l. (at profile)

AAR = 61 %

Variation of mass balance along a central flow line on Síðujökull is shown in Fig. 12. Snow accumulation was slightly over average in the accumulation zone but up to about 1. std. at the lower sites.

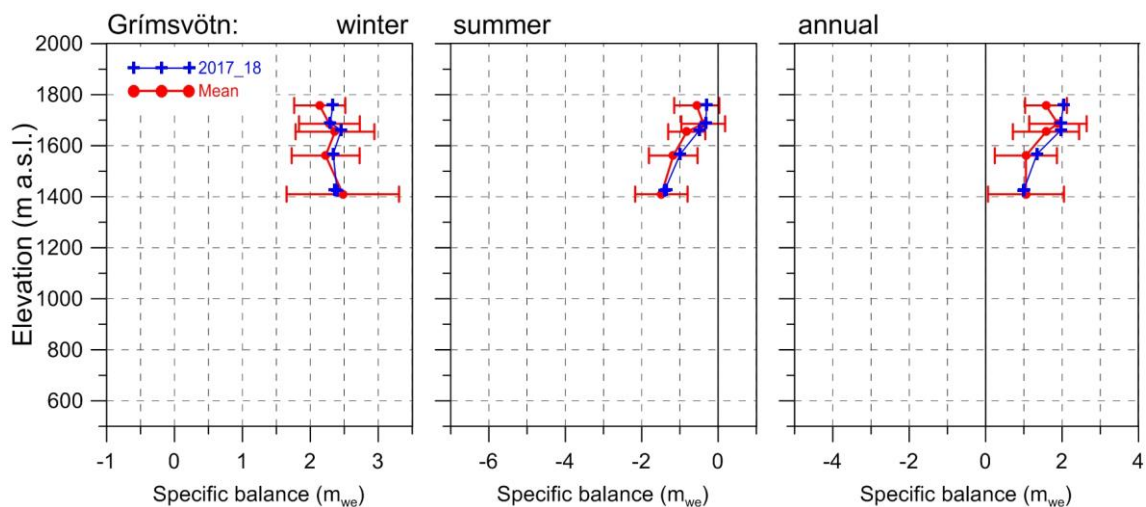


Figure 13. Mass balance at a central flow line towards Grímsvötn 2017_18 and average mass balance 1991_92 to 2016_17.

The total winter balance was 15% over the average (past decade). Summer mass loss was about 1 std. less than average. The total summer balance was negative by ~70% of the average of the survey period. The net balance was negative but 1 m less than in an average year of the survey period, only ~13% of the average of last decade.

3.2.6 Grímsvötn-Gjálp

Area = 174 km²
 $B_w = 0,32 \text{ km}^3_{we}; b_w = 2,38 \text{ m}_{we}$
 $B_s = -0,11 \text{ km}^3_{we}; b_s = -0,82 \text{ m}_{we}$
 $B_n = 0,21 \text{ km}^3_{we}; b_n = 1,56 \text{ m}_{we}$

Variation of mass balance close to a central flow line from Bárðarbunga towards Grímsvötn center is shown in Fig. 13. Snow accumulation was close to average at all survey sites except the highest, and the same applies to both summer and net balance. Total value of all the mb components were within 5% of the average of the survey period (since 1991-92). In addition to surface melt in summer geothermal melt in the Grímsvötn area in the order of 0,2 km² annually, this is not accounted for here.

3.3 The mass balance record for Vatnajökull.

From the digital maps the total volumes of winter, summer and net balance for Vatnajökull (and selected outlets) have been calculated by integration (appendix D, gives balance values as a function of elevation) and are as follows:

$B_w = 13,99 \text{ km}^3_{we}; b_w = 1,76 \text{ m}_{we}$
 $B_s = -14,07 \text{ km}^3_{we}; b_s = -2,77 \text{ m}_{we}$
 $B_n = -0,08 \text{ km}^3_{we}; b_n = -0,01 \text{ m}_{we}$
AAR = 62%

The weather in the autumn and first winter months 2017-18, was wet and rather warm, not much snowfall below ~1000 m. The latter half winter into,

especially February and May were also relatively warm with more than average precipitation. The spring was relatively cold and dry.

The total winter balance was ~10% higher than average (over the observation period from 1991_92, Fig. 14). The zero mass balance turnover for Vatnajökull (current topography) is close to 13,5 km³_{we} (1,7 m_{we}) and the winter balance 2017_18 is ~4% higher. First summer months were cold, calm and mostly dry, but cloudy, and even wet in the S and SW over Vatnajökull. Melting at lower ablation zone extended well into October and even November. This resulted in total melt

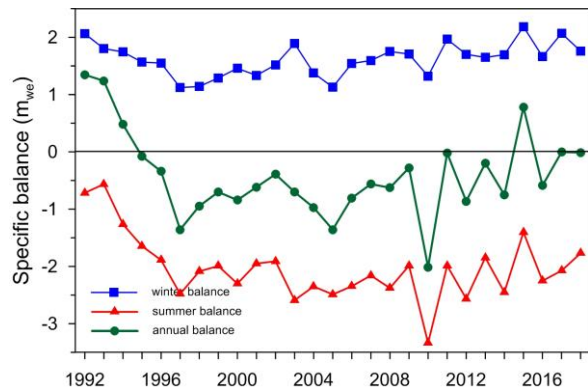


Figure 14. Specific mass balance record for Vatnajökull 1991_92 – 2017_18.

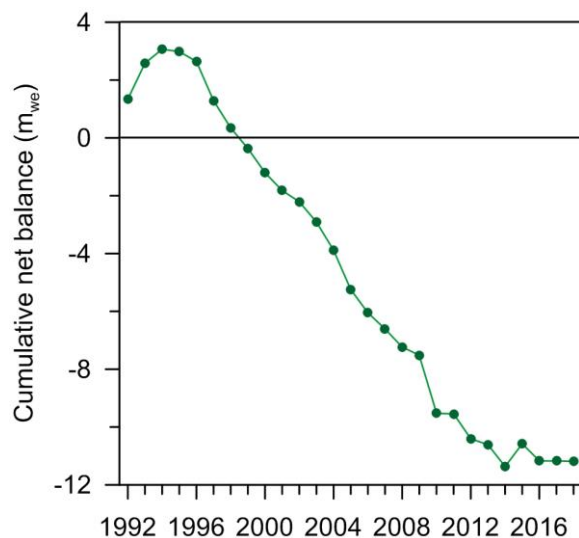


Figure 15. Cumulative specific mass balance of Vatnajökull 1991_92 – 2017_18.

by far less than average melt in the ablation zone (except in the North) but close to average in the accumulation zone. The total summer balance was negative but only ~80% of the average since 1995. As mentioned above, zero mass balance turnover for Vatnajökull (current topography) is close to 13,5 km³_{we} (1,7 m_{we}), the summer balance 2018 was -14.07 km³_{we} or ~4 % more loss than the zero balance turnover. The net balance was only marginally

negative this year, as last year, though last year turnover was ~ 2 km³ larger (15%) than 2017_18. The net balance has been negative since 1994_95 (except 2014_15).

However the ~20 year period of high mass loss seems to have halted, and currently Vatnajökull is close balance. The temporal variability of mass balance for different outlets is shown in Fig. 16. The variability of the winter balance is by far more

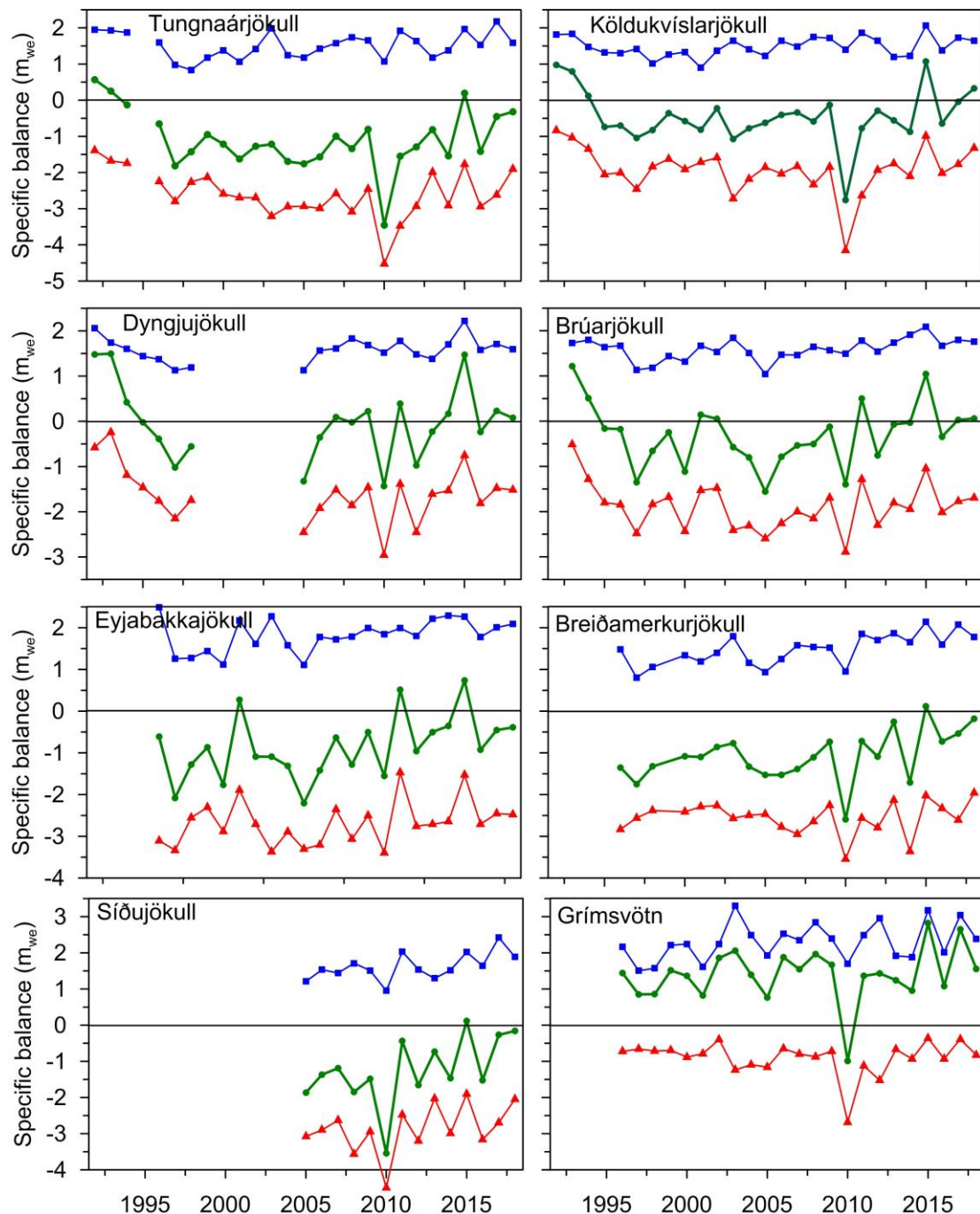


Figure 16. Specific mass balance record for Vatnajökull outlets 1991_92-2017_18.

prominent for the outlets closest to sea. That part of the glacier receives precipitation from all south and east wind directions, and thus has high snow accumulation in winters when the paths of the North Atlantic lows are just south and east of Iceland.

During the period of high net mass loss since 1994_95, the northern outlets have had several years of close to zero and positive mass balance.

The cumulative net balance curves for the outlets of Vatnajökull in Fig. 17 show that all outlets have been losing mass since 1994_95. The slope for mass loss is about $0,7 \text{ m}_{\text{we}}\text{a}^{-1}$ for the northern outlets but $1,5 \text{ m}_{\text{we}}\text{a}^{-1}$ for the south and western outlets.

In Fig. 18 the relation of the annual net balance to the accumulation area ratio (AAR) and equilibrium line altitude (ELA) is shown for different outlets over the survey period. The b_n -AAR gradient is similar for all outlets, about $0,5 \text{ m}_{\text{we}}$ for 10% change in AAR. The zero-balance AAR varies for different outlets from about 60-65%, similar for all outlets except for the southern outlet Breiðamerkurjökull.

Breiðamerkurjökull is far from equilibrium, the ablation area is too large. A large part of the outlet has carved 200-300 m through the former

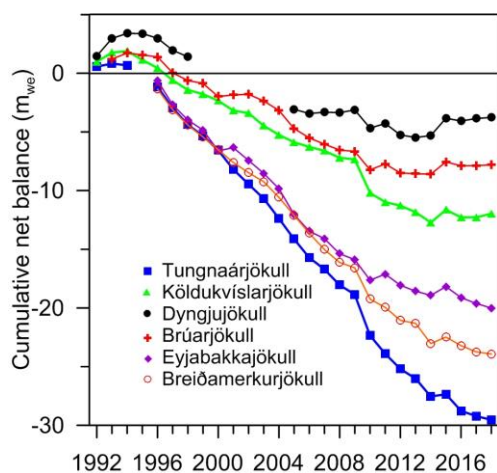


Figure 17. Cumulative specific surface mass balance for several of Vatnajökull outlets 1991_92 – 2017_18.

sediment bed, and the surface elevation has lowered accordingly. Breiðamerkurjökull has been retreating at a high rate for decades.

Similarly the zero-balance ELA varies from about 1000-1100 m a.s.l. for the southern outlets to 1400 m a.s.l. for the NW outlets. The b_n -ELA slope is similar for all outlets $-0,7 \text{ m}_{\text{we}}$ per 100 m, except Eyjabakkajökull with a slope of -1 m_{we} per 100.

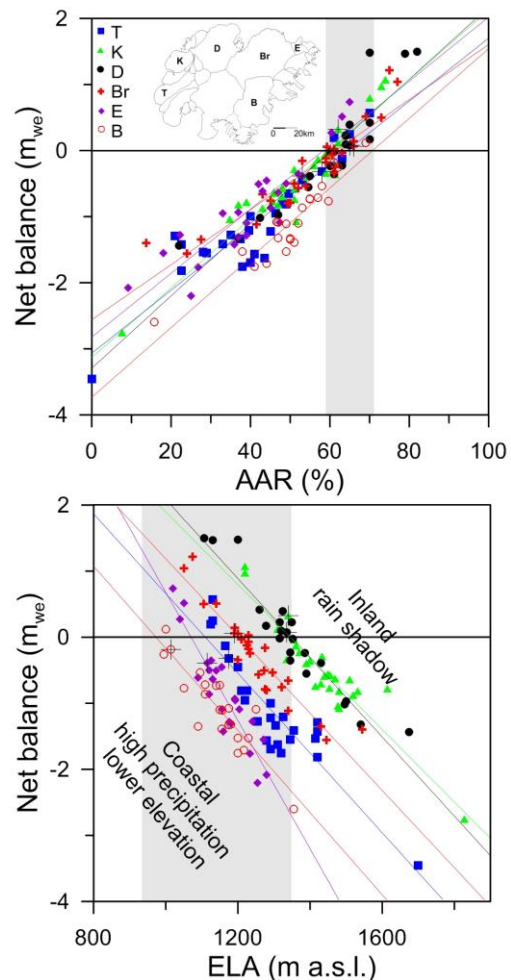


Figure 18. The relation between net annual balance (b_n) and accumulation area ratio (AAR) (upper) and b_n and equilibrium line altitude (ELA), for Vatnajökull outlets during the survey period. (This years points are marked with a black +).

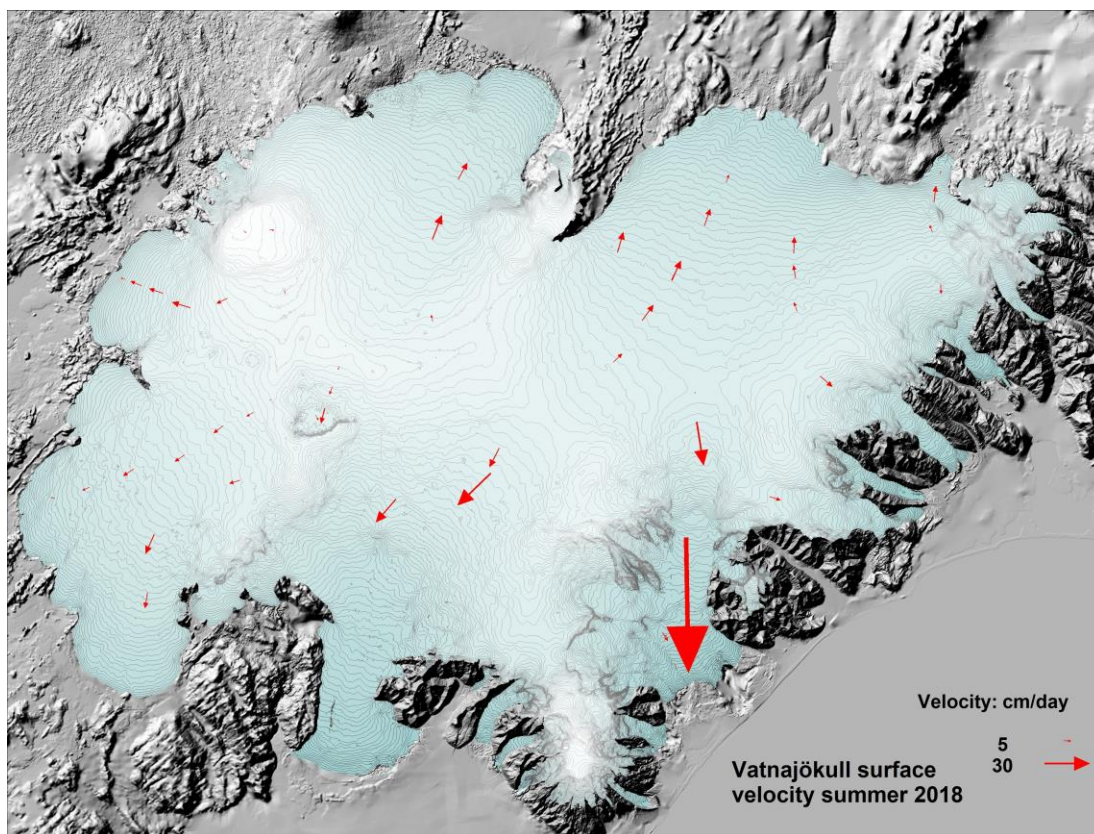


Figure 19. Average surface velocity at survey sites in 2017_18.

4. SURFACE VELOCITY MEASUREMENTS

The surface velocity of the glacier was calculated from DGPS (accuracy within 1 m), fast static (accuracy about 1 cm) and kinematic GPS (accuracy about 3 cm) positioning of the ablation stakes. All sites were surveyed in spring and autumn (most kinematic, some DGPS), and many also in June (kinematic), August (fast static) and October (kinematic). At a few sites stakes from previous years were found and resurveyed, making it possible to calculate surface velocity over a year or longer time span. The average summer surface velocity is shown on Figure 19.

At sites close to the glacier edge very small horizontal movement is measured. This indicates that the glacier snouts are almost stagnant. In the centre areas of some of the outlets

especially close to the equilibrium line, there is an increase in velocity during summer compared to winter. The summer velocity is of the order of two-fold the winter velocity. This suggests that basal sliding is increased in the melting season, and is of the same magnitude as the deformation velocity. To better understand this continuous GPS has been run during summer at several sites.

From previous velocity measurements, surging of outlets has been predicted. Currently increase in velocity at sites D05 and D07 suggests Dyngjufjökull may surge within a few years.

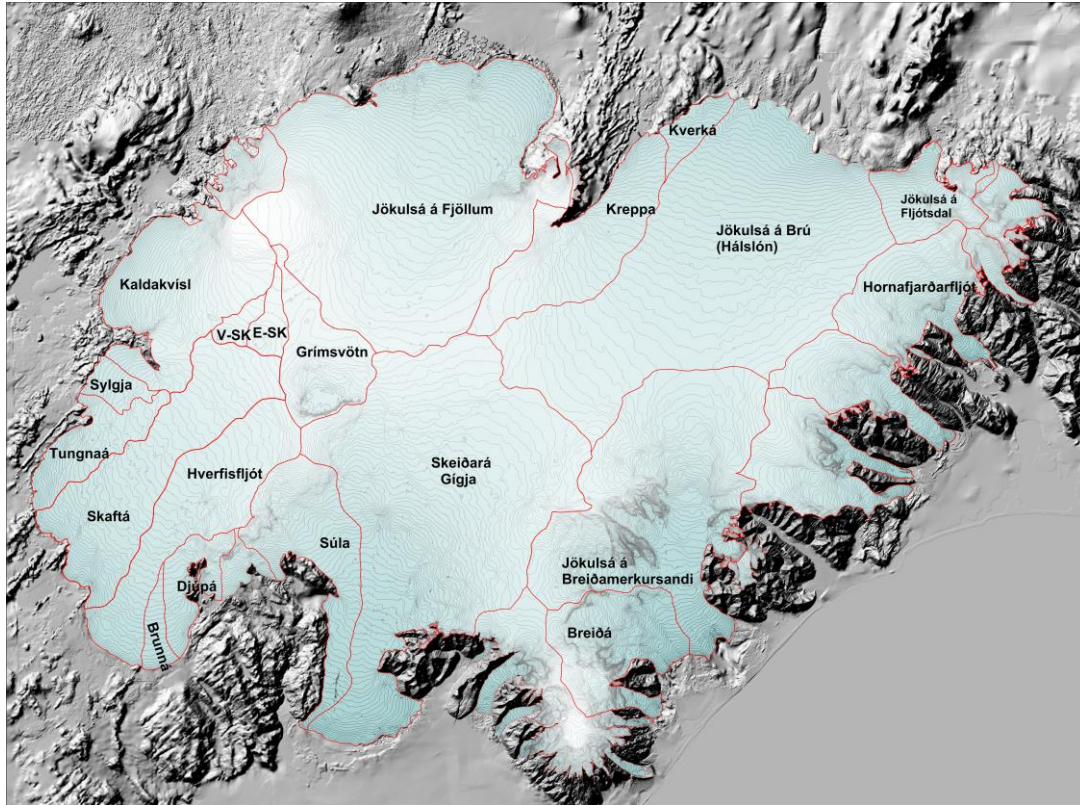


Figure 20. Water divides and drainage basins of selected rivers draining water from Vatnajökull.

5. Melt water runoff.

Water divides and drainage basins for rivers draining water from Vatnajökull have been defined from water pressure potential maps. The potential maps were produced from existing surface (year 2010) and bedrock digital elevation models.

Figure 20 shows the water divides and drainage areas for selected rivers draining meltwater from Vatnajökull. The summer balance over the water basin is an estimate of meltwater contribution to rivers and groundwater storage. This estimate, however, does not include precipitation that falls as rain on the glacier, nor snow that falls and melts during the summer. The meltwater contribution can be compared with river runoff at stream flow gauges closest to the glacier. For this comparison, we define the glaciological year from the start of October to the end of September and the period draining meltwater from the

glacier during the summer from June through September. It would be misleading to include May in the summer period because runoff from

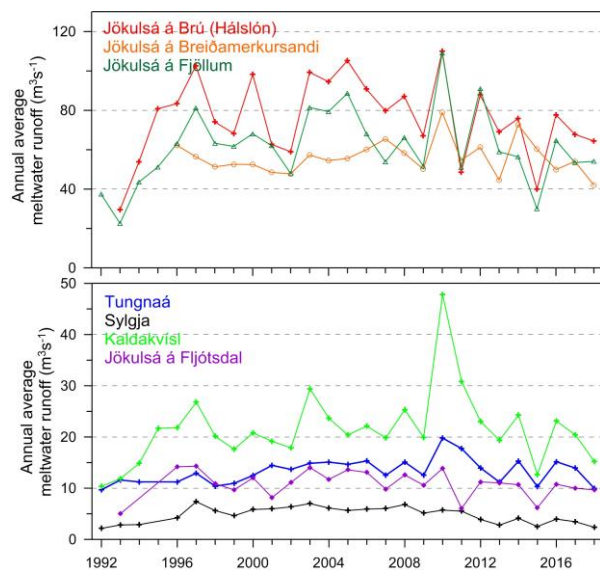


Figure 21. The temporal variation of average annual meltwater runoff to selected river catchments.

Table I. Melt water drainage to selected rivers.

Water Catchment:	Area (km ²)	ΣQ_s (10 ⁶ m ³)	Q_s (m ³ s ⁻¹)	Q_a (m ³ s ⁻¹)	q_s (ls ⁻¹ km ⁻²)
Vatnajökull	7890,0	14096,0	1337,3	447,0	56,7
Tungnaá	121,8	314,1	29,8	10,0	81,8
Sylgja	39,7	74,2	7,0	2,4	59,3
Kaldakvísl	367,9	479,9	45,5	15,2	41,4
Jokulsa a Fjöllum	1188,3	1706,2	161,9	54,1	45,5
Kreppa	291,2	365,8	34,7	11,6	39,8
Kverka	47,0	203,9	19,3	6,5	137,6
Jokulsa a Brú	1214,8	2031,6	192,7	64,4	53,0
Jökulsá á Fljótssdal	130,7	305,6	29,0	9,7	74,1
Jökulsá í Lóni	101,3	176,0	16,7	5,6	55,1
Hornafjarðarfjót	239,1	589,1	55,9	18,7	78,1
Jökulsá á Breiðamerkursandi	739,5	1324,5	125,7	42,0	56,8
Breiðá-Fjallsá	234,6	641,3	60,8	20,3	86,7
Skeiðará-Gígja	1165,2	2078,1	197,1	65,9	56,6
Súla	255,8	641,1	60,8	20,3	79,5
Brunná	35,8	122,8	11,6	3,9	108,8
Djúpá	83,7	209,0	19,8	6,6	79,2
Hverfisfjót	317,7	506,7	48,1	16,1	50,6
Skaftá	394,9	719,4	68,2	22,8	57,8
Grímsvötn	173,3	124,6	11,8	4,0	22,8
Eystri Skaftárketill	39,3	15,0	1,4	0,5	12,1
Vestari Skaftárketill	25,1	9,2	0,9	0,3	11,6
Hólmsá	164,8	313,3	29,7	9,9	60,3
Heinabergsvötn	229,5	465,9	44,2	14,8	64,4
Skjálfafljót	97,2	102,1	9,7	3,2	33,3

ΣQ_s : total summer melt water; Q_s : average runoff (averaged over summer, 4 months, June – September)
 Q_a : average runoff (averaged over a whole year); q_s : average runoff per km² (averaged over a whole year)

the glacier melt in May is delayed due to refreezing during elimination of the cold wave and because of the contribution of the spring melt from the highlands to the runoff. Some melting also occurs during winter, especially in the low snouts of the southern outlets.

Average melt water runoff to different rivers is given in Table I, and temporal variation of the average meltwater runoff in Fig. 21. The average specific runoff (q_s) differs from basin to basin from ~10 to ~140 ls⁻¹km⁻². This is mainly due to different elevation distributions, for example, the water drainage basins for Tungnaá and Kverka are within the ablation area, while that of Grímsvötn and

Skaftárkatlar are high in the accumulation zone.

6. Conclusions

In the glaciological year 2017_18 the winter balance for Vatnajökull exceeded the average, over the observation period from 1991_92, by ~10%.

The total summer mass loss was about 80% of the average since 1995. The net balance was negative as it has been since 1994_95 (except 2014_15), but now only marginally so, just as last year 2016_17.

The about 20 year period of high mass loss seems to have halted; the past few years have all had net balance close to zero, and there has been a positive trend in the net balance since about 2009, although with high variability.

The 2017_18 close to zero balance is primarily explained by summer mass loss less than the average of the survey period.

The total mass loss over the 27 year survey period is 11,2 m_{we} (ice volume of ~99 km³) since 1991_92 (or since 1994_95, 14,2 m_{we}, ice volume of 126 km³). The volume loss since 1991_92 amounts to ~3% of total ice volume (~4% since 1994_95).

Glacier meltwater runoff in summer

2018 (estimated from summer surface balance only, summer rain and snow that falls and melts during summer, calving and geothermal melting, is not included; averages refer to the survey period of each outlet): to Tungnaá 68% of the average, 69 % of the average to Kaldakvísl, 89% of the average to Jökulsá á Fjöllum, 91% of the average to Háslón, 90% of average to Jökulsá í Fljótsdal and 76% of the average to Jökulsá á Breiðamerkursandi.

Surface velocity measurements suggest that Dyngjujökull is in first phase of a surge, and will complete a surge cycle within the next few years.

Mass balance summary 2017_18:

$$\begin{aligned} B_w &= 13,99 \text{ km}^3_{we} \\ B_s &= -14,07 \text{ km}^3_{we} \\ B_n &= -0,08 \text{ km}^3_{we} \\ AAR &= 62\% \end{aligned}$$

Specific Values:

$$\begin{aligned} b_w &= 1,76 \text{ m}_{we} \\ b_s &= -2,77 \text{ m}_{we} \\ b_n &= -0,01 \text{ m}_{we} \end{aligned}$$

Appendix A: Mass balance at measurement sites 2017_18.

b_w : specific winter balance, b_s : specific summer balance, b_n : specific net balance,
 l_a : new snow in autumn (all in water equivalent).

Site	Position			Elevation (m a.s.l.)	Date in spring	Date in autumn	b_w (m)	b_s (m)	b_n (m)	l_a (m)	
	Latitude	Longitude									
B09-18	64	45,040	16	5,464	725,9	20180510	20181009	0,18	-5,121	-4,945	föl
B10-18	64	43,686	16	6,700	785,3	20180510	20181009	0,43	-4,750	-4,322	föl
B11-18	64	40,969	16	10,466	952,6	20180510	20181009	0,93	-3,477	-2,545	0,09
B12-18	64	38,267	16	14,130	1077,9	20180510	20181009	0,88	-2,338	-1,458	0,14
B13-18	64	34,537	16	19,696	1219,5	20180510	20181009	1,58	-1,202	0,378	0,19
B14-18	64	31,634	16	24,708	1321,4	20180509	20181009	1,86	-1,093	0,771	0,24
B15-18	64	28,489	16	30,020	1405,1	20180509	20181009	1,92	-0,720	1,200	0,2
B16-18	64	24,127	16	40,860	1530,3	20180509	20181009	2,60	-0,526	2,074	0,29
B17-17	64	36,736	16	28,800	1215,9	20180510	20181009	1,29	-1,344	-0,057	0,2
Br1-18	64	5,835	16	19,712	116,3	20180508	20181010	-0,55	-5,310	-5,860	föl
Br2-18	64	6,368	16	22,537	201,1	20180508	20180000	-0,60	-6,230	-6,830	0
Br3-18	64	8,465	16	24,041	381,1	20180508	20180000	0,00	-3,950	-3,950	0
Br4-18	64	10,967	16	20,113	528,9	20180514	20180000	0,10			0
Br7-18	64	22,141	16	16,951	1249,0	20180509	20181009	2,77	-1,340	1,427	0,25
B07-18	64	25,795	16	17,455	1360,1	20180509	20181009	2,38	-1,184	1,200	0,21
BB0-18	64	22,707	16	5,049	1521,7	20180508	20181008	2,65	-0,544	2,101	0,4
Bru-18	64	40,986	15	55,316	750,1	20180508	20181009	0,65	-5,645	-4,996	0,01
Bud-18	64	35,992	15	59,897	1137,8	20180508	20181009	1,57	-1,505	0,065	0,32
gb2-18	64	34,102	16	0,015	1204,7	20180508	20181009	1,73	-1,528	0,199	0,35
B18-18	64	31,584	16	0,126	1315,7	20180508	20181009	2,92	-1,020	1,900	0,39
B19-18	64	27,996	15	55,981	1441,1	20180508	20181009	2,91	-0,583	2,331	0,35
BB0-18	64	22,707	16	5,049	1521,7	20180508	20181008	2,65	-0,544	2,101	0,4
D05-18	64	42,224	16	54,697	1204,9	20180511	20181010	0,80	-2,279	-1,476	0,18
D07-18	64	38,285	16	59,270	1377,7	20180511	20181010	1,54	-1,090	0,446	0,3
D09-18	64	31,794	17	0,600	1587,0	20180511	20181010	2,27	-0,457	1,813	0,27
D12-18	64	28,977	17	0,178	1651,0	20180511	20181010	2,28	-0,330	1,954	0,3
E01-18	64	40,626	15	34,869	771,0	20180508	20181009	0,98	-5,327	-4,347	0,05
E02-18	64	39,128	15	35,984	953,7	20180508	20181009	1,35	-3,690	-2,342	0,05
E03-18	64	36,664	15	36,924	1189,8	20180508	20181009	2,56	-1,527	1,031	0,32
E04-18	64	34,954	15	37,111	1290,4	20180508	20181009	2,73	-0,676	2,058	0,3
K01-18	64	35,167	17	51,816	1052,9	20180512	20181010	1,35	-3,591	-2,241	0,05
K02-18	64	34,810	17	49,676	1174,4	20180512	20181010	1,20	-2,046	-0,849	0,14
K03-18	64	34,246	17	46,375	1297,1	20180512	20181010	1,32	-1,554	-0,237	0,2
K04-18	64	33,209	17	42,243	1489,9	20180512	20181010	1,69	-0,884	0,810	0,25
K05-18	64	33,445	17	35,430	1682,3	20180511	20181010	1,98	-0,225	1,753	0,26
K06-18	64	38,351	17	31,356	1948	20180605	20181010	2,74	0,280	3,019	0,51
K07-18	64	29,115	17	42,043	1535	20180512	20181010	1,83	-0,780	1,045	0,25
S01-18	64	7,002	17	49,967	724,1	20180512	20181010	0,96	-3,651	-2,691	0,16
S02-18	64	12,159	17	48,965	1006	20180512	20181010	2,06	-2,420	-0,360	0,21
S04-18	64	16,186	17	48,192	1161	20180512	20181010	1,97	-1,548	0,417	0,21
S05-18	64	20,498	17	33,998	1453,0	20180512	20181010	2,38	-0,820	1,562	0,25
Haab-18	64	20,963	17	24,119	1734	20180513	20181010	3,13	0,160	3,285	0,32

T01-18	64	19,545	18	7,077	778,2	20180512	20181010	0,14	-4,775	-4,638	föl
T02-18	64	19,598	18	4,017	927,1	20180512	20181010	1,65	-2,901	-1,251	0,18
T03-18	64	20,205	17	58,591	1072,0	20180512	20181010	1,17	-2,250	-1,080	0,16
T04-18	64	21,324	17	51,515	1220,8	20180512	20181010	1,94	-1,459	0,479	0,17
T05-18	64	22,267	17	43,007	1347,0	20180512	20181010	1,87	-1,090	0,780	0,22
T06-18	64	24,261	17	36,522	1469,8	20180513	20181010	2,04	-0,675	1,365	0,21
T07-18	64	25,293	17	31,206	1565,7	20180513	20181010	2,33	-0,445	1,881	0,22
T08-18	64	26,295	17	27,759	1639,1	20180513	20181010	2,23	-0,390	1,837	0,23
Borth-a	64	25,044	17	19,178	1427,9	20180605	20181010	2,36	-1,359	1,001	0,18
Bor-18	64	24,941	17	20,143	1423,8	20180604	20181010	2,39	-1,402	0,991	0,18
G02-18	64	26,848	17	17,727	1567,0	20180604	20181010	2,33	-0,991	1,344	0,28
G03-18	64	28,436	17	16,329	1660,6	20180605	20181010	2,45	-0,487	1,966	0,32
G04-18	64	30,024	17	15,042	1689,1	20180605	20181010	2,29	-0,327	1,966	0,32
Go1-18	64	33,974	17	24,958	1761,5	20180605	20181010	2,33	-0,296	2,038	0,33
Hof01-18	64	32,333	15	35,845	1143,9	20180508	20181009	2,70	-1,309	1,388	0,25
FI01-18	64	26,157	15	55,625	1350,0	20180508	20181009	2,96	-1,049	1,911	0,39
Skf01-18	64	17,986	16	5,008	1285,9	20180508	20181008	3,32	-1,006	2,314	0,32
Skf00-18	64	15,460	15	54,064	952,2	20180507	20181008	1,64	-1,91	-0,271	0,26
Barc-18	64	38,427	17	26,868	1893,8	20180605	20181010	2,41	0,490	2,904	0,39
Ske02-18	64	18,161	17	9,179	1209,0	20180513	20181009	1,58	-1,751	-0,173	0,12
Ske03-18	64	17,801	17	0,004	1254,7	20180509	20180000	1,77			
Ske04-18	64	19,492	16	54,514	1368,3	20180509	20181009	1,87	-1,480	0,392	0,22
Ske05-18	64	21,704	16	51,017	1437	20180509	20181009	2,06	-0,910	1,146	0,13
Herm-18	64	7,316	16	43,381	1310	20180603	20180000	3,264			
TjSk-18	64	2,505	16	39,629	1831	20180603	20180000	4,646			
Or02-18	63	59,611	16	37,980	1796	20180604	20180000	5,722			
Or06-18	63	59,100	16	39,709	1808	20180604	20180000	5,327			
Or01-18	63	59,900	16	39,200	1822	20180604	20180000	6,094			
Or05-18	64	0,179	16	39,790	1833	20180604	20180000	5,694			
Or03-18	64	0,271	16	37,942	1843	20180605	20180000	5,187			
Or07-18	64	0,419	16	39,041	1853	20180603	20180000	6,686			
Or04-18	64	0,974	16	39,109	1876	20180603	20180000	5,424			

Appendix B: Balance distribution by elevation in 2017_18.

ΔS : area in elevation range, $\Sigma\Delta S$: cumulative area above given elevation, b_w : specific winter balance, b_s : specific summer balance. b_n : specific winter balance, ΔB_w : winter balance at a given elevation range, $\Sigma\Delta B_w$: cumulative winter balance above given elevation, ΔB_s summer balance at a given elevation range, $\Sigma\Delta B_s$: cumulative summer balance above given elevation, ΔB_n : net annual balance in a given elevation range, ΣB_n : cumulative net annual balance above given elevation.

Vatnajökull

Elevation (m a.s.l.)			ΔS (km^2)	$\Sigma\Delta S$ (km^2)	b_w (mm)	b_s (mm)	b_n (mm)	ΔB_w ($10^6 m^3$)	$\Sigma\Delta B_w$ ($10^6 m^3$)	ΔB_s ($10^6 m^3$)	$\Sigma\Delta B_s$ ($10^6 m^3$)	ΔB_n ($10^6 m^3$)	ΣB_n ($10^6 m^3$)
2000	2050	2025	0,4	0,4	4731	307	5039	2,1	2,1	0,1	0,1	2,3	2,3
1950	2000	1975	8,8	9,2	2945	235	3181	25,8	27,9	2,1	2,2	27,9	30,1
1900	1950	1925	36,6	45,8	2668	263	2932	97,6	125,5	9,7	11,9	107,2	137,4
1850	1900	1875	47,4	93,2	2803	193	2996	133	258,5	9,2	21,0	142,1	279,5
1800	1850	1825	47,0	140,2	3106	51	3157	145,9	404,4	2,4	23,4	148,3	427,8
1750	1800	1775	54,5	194,7	2736	-90	2645	149,3	553,6	-4,9	18,5	144,3	572,1
1700	1750	1725	104,3	299,0	2462	-226	2236	256,9	810,6	-23,6	-5,2	233,3	805,4
1650	1700	1675	222,4	521,4	2385	-355	2029	530,5	1341,1	-79,1	-84,3	451,4	1256,8
1600	1650	1625	373,0	894,4	2382	-422	1959	888,7	2229,8	-157,7	-242,0	731,0	1987,8
1550	1600	1575	353,6	1248,0	2343	-493	1849	828,6	3058,4	-174,6	-416,6	653,9	2641,7
1500	1550	1525	420,6	1668,6	2306	-585	1720	970	4028,4	-246,3	-663,0	723,6	3365,4
1450	1500	1475	453,2	2121,8	2243	-699	1544	1017	5045,2	-316,8	-979,8	700,0	4065,4
1400	1450	1425	503,8	2625,6	2260	-844	1416	1139	6184,3	-425,5	-1405,3	713,6	4779,0
1350	1400	1375	548,7	3174,3	2266	-1019	1246	1244	7427,9	-559,6	-1964,8	684,1	5463,1
1300	1350	1325	540,9	3715,2	2233	-1166	1066	1208	8635,8	-631,0	-2595,9	576,8	6039,9
1250	1300	1275	512,0	4227,2	2136	-1281	855	1094	9729,9	-656,0	-3251,9	438,1	6478,0
1200	1250	1225	453,3	4680,5	1920	-1447	473	870,7	10601	-656,0	-3907,9	214,7	6692,7
1150	1200	1175	403,5	5084,0	1729	-1682	46	697,7	11298	-679,0	-4586,8	18,8	6711,5
1100	1150	1125	362,5	5446,5	1620	-1977	-357	587,4	11886	-716,9	-5303,7	-129,5	6582,0
1050	1100	1075	323,6	5770,1	1499	-2303	-803	485,2	12371	-745,3	-6049,1	-260,1	6321,9
1000	1050	1025	301,1	6071,2	1374	-2631	-1256	413,7	12785	-792,1	-6841,2	-378,4	5943,4
950	1000	975	270,8	6342,0	1233	-2915	-1681	334,2	13119	-789,6	-7630,8	-455,5	5488,0
900	950	925	238,3	6580,3	1114	-3145	-2030	265,7	13385	-749,6	-8380,4	-483,9	5004,1
850	900	875	210,2	6790,5	962	-3406	-2444	202,2	13587	-716,2	-9096,6	-513,9	4490,2
800	850	825	192,1	6982,6	822	-3674	-2852	158	13745	-706,0	-9802,5	-548,0	3942,2
750	800	775	174,8	7157,4	675	-3966	-3291	118	13863	-693,3	-10495,9	-575,3	3366,9
700	750	725	141,2	7298,6	609	-4010	-3400	86,1	13949	-566,2	-11062,1	-480,1	2886,8
650	700	675	121,3	7419,9	561	-3967	-3406	68,1	14017	-481,2	-11543,3	-413,1	2473,7
600	650	625	74,6	7494,5	456	-3726	-3270	34	14051	-278,1	-11821,4	-244,0	2229,7
550	600	575	65,8	7560,3	286	-3670	-3384	18,8	14070	-241,6	-12063,0	-222,8	2006,9
500	550	525	48,0	7608,3	189	-3791	-3602	9,1	14079	-181,8	-12244,8	-172,8	1834,1
450	500	475	40,4	7648,7	62	-3954	-3891	2,5	14082	-159,8	-12404,6	-157,2	1676,9
400	450	425	44,5	7693,2	-17	-4154	-4172	-0,8	14081	-185,0	-12589,6	-185,8	1491,1
350	400	375	40,0	7733,2	-121	-4586	-4708	-4,9	14076	-183,5	-12773,1	-188,4	1302,7
300	350	325	38,1	7771,3	-214	-5021	-5235	-8,2	14068	-191,2	-12964,4	-199,4	1103,3
250	300	275	36,6	7807,9	-280	-5387	-5668	-10,3	14057	-197,3	-13161,7	-207,6	895,7
200	250	225	37,5	7845,4	-355	-5776	-6131	-13,3	14044	-216,4	-13378,1	-229,8	665,9
150	200	175	32,5	7877,9	-449	-6210	-6660	-14,6	14030	-201,5	-13579,6	-216,1	449,8
100	150	125	28,3	7906,2	-534	-6542	-7077	-15,1	14014	-185,2	-13764,9	-200,4	249,5
50	100	75	25,9	7932,1	-605	-6824	-7430	-15,7	13999	-176,7	-13941,6	-192,4	57,1
0	50	25	18,3	7950,4	-688	-7120	-7808	-12,6	13986	-130,4	-14071,9	-143,0	-85,9

Tungnaárjökull

Elevation (m a.s.l.)			ΔS (km^2)	$\Sigma \Delta S$ (km^2)	b_w (mm)	b_s (mm)	b_n (mm)	ΔB_w (10^6m^3)	$\Sigma \Delta B_w$ (10^6m^3)	ΔB_s (10^6m^3)	$\Sigma \Delta B_s$ (10^6m^3)	ΔB_n (10^6m^3)	ΣB_n (10^6m^3)
1650	1700	1675	1,8	1,8	2176	-468	1708	4	4	-0,9	-0,9	3,2	3,2
1600	1650	1625	12,7	14,5	2187	-406	1781	27,9	31,9	-5,2	-6,0	22,7	25,9
1550	1600	1575	15,7	30,2	2136	-427	1709	33,5	65,4	-6,7	-12,7	26,8	52,7
1500	1550	1525	15,5	45,7	2079	-526	1552	32,3	97,7	-8,2	-20,9	24,1	76,8
1450	1500	1475	18,4	64,1	2006	-657	1349	36,8	134,5	-12,1	-33,0	24,8	101,5
1400	1450	1425	23,0	87,1	1990	-820	1169	45,7	180,2	-18,8	-51,8	26,9	128,4
1350	1400	1375	21,4	108,5	1951	-988	963	41,7	221,9	-21,1	-72,9	20,6	149,0
1300	1350	1325	27,5	136,0	1912	-1136	775	52,6	274,5	-31,3	-104,2	21,3	170,3
1250	1300	1275	21,1	157,1	1902	-1279	622	40,2	314,7	-27,0	-131,2	13,1	183,4
1200	1250	1225	23,1	180,2	1857	-1451	406	42,9	357,6	-33,5	-164,7	9,4	192,8
1150	1200	1175	21,0	201,2	1780	-1659	121	37,4	395	-34,8	-199,6	2,5	195,4
1100	1150	1125	18,4	219,6	1647	-1925	-278	30,3	425,2	-35,4	-235,0	-5,1	190,3
1050	1100	1075	19,1	238,7	1519	-2229	-709	29,1	454,3	-42,7	-277,6	-13,6	176,7
1000	1050	1025	17,5	256,2	1390	-2508	-1117	24,3	478,6	-43,8	-321,4	-19,5	157,2
950	1000	975	17,3	273,5	1207	-2816	-1608	20,9	499,5	-48,7	-370,1	-27,8	129,3
900	950	925	16,4	289,9	993	-3209	-2215	16,3	515,8	-52,7	-422,8	-36,4	93,0
850	900	875	13,5	303,4	742	-3663	-2920	10	525,8	-49,5	-472,3	-39,4	53,5
800	850	825	14,1	317,5	525	-4234	-3709	7,4	533,2	-59,5	-531,8	-52,2	1,4
750	800	775	11,4	328,9	285	-4825	-4540	3,2	536,5	-54,9	-586,8	-51,7	-50,3
700	750	725	7,8	336,7	148	-5179	-5031	1,2	537,6	-40,4	-627,1	-39,2	-89,5
650	700	675	3,7	340,4	104	-5378	-5273	0,4	538	-19,9	-647,0	-19,5	-109,0

Sylgjujökull

Elevation (m a.s.l.)			ΔS (km^2)	$\Sigma \Delta S$ (km^2)	b_w (mm)	b_s (mm)	b_n (mm)	ΔB_w (10^6m^3)	$\Sigma \Delta B_w$ (10^6m^3)	ΔB_s (10^6m^3)	$\Sigma \Delta B_s$ (10^6m^3)	ΔB_n (10^6m^3)	ΣB_n (10^6m^3)
1600	1650	1625	1,7	1,7	2007	-402	1605	3,4	3,4	-0,7	-0,7	2,7	2,7
1550	1600	1575	5,5	7,2	1962	-460	1502	10,7	14,1	-2,5	-3,2	8,2	10,9
1500	1550	1525	18,6	25,8	1854	-625	1228	34,5	48,6	-11,6	-14,8	22,8	33,8
1450	1500	1475	13,2	39,0	1818	-747	1070	24	72,6	-9,9	-24,7	14,1	47,9
1400	1450	1425	8,3	47,3	1825	-838	987	15,1	87,7	-6,9	-31,6	8,2	56,1
1350	1400	1375	5,6	52,9	1826	-953	873	10,2	97,9	-5,3	-36,9	4,9	60,9
1300	1350	1325	5,2	58,1	1809	-1108	700	9,3	107,2	-5,7	-42,6	3,6	64,5
1250	1300	1275	10,1	68,2	1776	-1278	498	17,9	125,1	-12,8	-55,5	5,0	69,6
1200	1250	1225	12,0	80,2	1712	-1474	238	20,6	145,6	-17,7	-73,2	2,9	72,4
1150	1200	1175	13,6	93,8	1620	-1675	-54	22,1	167,7	-22,8	-96,1	-0,7	71,7
1100	1150	1125	12,8	106,6	1486	-1868	-381	19	186,7	-23,8	-119,9	-4,9	66,8
1050	1100	1075	12,3	118,9	1331	-2155	-823	16,3	203	-26,4	-146,3	-10,1	56,7
1000	1050	1025	10,9	129,8	1160	-2776	-1615	12,6	215,6	-30,1	-176,4	-17,5	39,2
950	1000	975	3,8	133,6	1040	-2901	-1860	3,9	219,6	-11,0	-187,4	-7,1	32,1
900	950	925	1,7	135,3	885	-2818	-1932	1,5	221,1	-4,8	-192,2	-3,3	28,9
850	900	875	0,3	135,6	753	-2998	-2244	0,2	221,3	-1,0	-193,2	-0,7	28,1

Köldukvísarljökul

Elevation (m a.s.l.)			ΔS (km^2)	$\Sigma \Delta S$ (km^2)	b_w (mm)	b_s (mm)	b_n (mm)	ΔB_w ($10^6 m^3$)	$\Sigma \Delta B_w$ ($10^6 m^3$)	ΔB_s ($10^6 m^3$)	$\Sigma \Delta B_s$ ($10^6 m^3$)	ΔB_n ($10^6 m^3$)	ΣB_n ($10^6 m^3$)
1950	2000	1975	0,8	0,8	2577	277	2855	2,1	2,1	0,2	0,2	2,4	2,4
1900	1950	1925	13,9	14,7	2463	268	2732	34,3	36,5	3,7	4,0	38,1	40,4
1850	1900	1875	6,4	21,1	2333	144	2477	14,9	51,4	0,9	4,9	15,8	56,3
1800	1850	1825	6,0	27,1	2265	55	2321	13,7	65	0,3	5,2	14,0	70,3
1750	1800	1775	10,3	37,4	2258	-39	2219	23,3	88,3	-0,4	4,8	22,9	93,1
1700	1750	1725	17,0	54,4	2122	-151	1971	36	124,4	-2,6	2,3	33,5	126,6
1650	1700	1675	15,9	70,3	1974	-270	1704	31,4	155,8	-4,3	-2,0	27,1	153,7
1600	1650	1625	14,1	84,4	1883	-394	1488	26,6	182,4	-5,6	-7,6	21,0	174,8
1550	1600	1575	18,7	103,1	1809	-539	1270	33,8	216,2	-10,1	-17,7	23,7	198,5
1500	1550	1525	20,3	123,4	1724	-698	1025	35	251,2	-14,2	-31,9	20,8	219,3
1450	1500	1475	19,4	142,8	1652	-809	843	32,1	283,2	-15,7	-47,6	16,4	235,7
1400	1450	1425	15,3	158,1	1572	-943	628	24	307,2	-14,4	-62,0	9,6	245,3
1350	1400	1375	15,1	173,2	1474	-1127	346	22,3	329,5	-17,0	-79,0	5,2	250,5
1300	1350	1325	17,3	190,5	1391	-1349	41	24,1	353,6	-23,3	-102,4	0,7	251,2
1250	1300	1275	18,0	208,5	1341	-1580	-239	24,1	377,7	-28,4	-130,8	-4,3	246,9
1200	1250	1225	17,4	225,9	1324	-1807	-482	23	400,7	-31,4	-162,2	-8,4	238,5
1150	1200	1175	16,3	242,2	1314	-2150	-835	21,5	422,2	-35,1	-197,3	-13,6	224,9
1100	1150	1125	14,8	257,0	1297	-2754	-1456	19,2	441,3	-40,7	-238,0	-21,5	203,4
1050	1100	1075	13,4	270,4	1264	-3337	-2072	16,9	458,3	-44,7	-282,7	-27,8	175,6
1000	1050	1025	10,5	280,9	1210	-3800	-2590	12,7	471	-40,0	-322,7	-27,3	148,3
950	1000	975	9,7	290,6	1150	-4124	-2974	11,1	482,1	-39,8	-362,5	-28,7	119,6
900	950	925	6,3	296,9	1102	-4324	-3221	7	489,1	-27,4	-390,0	-20,4	99,2
850	900	875	0,9	297,8	1074	-4475	-3400	0,9	490,1	-3,9	-393,9	-3,0	96,2

Dyngjujökull

Elevation (m a.s.l.)			ΔS (km^2)	$\Sigma \Delta S$ (km^2)	b_w (mm)	b_s (mm)	b_n (mm)	ΔB_w ($10^6 m^3$)	$\Sigma \Delta B_w$ ($10^6 m^3$)	ΔB_s ($10^6 m^3$)	$\Sigma \Delta B_s$ ($10^6 m^3$)	ΔB_n ($10^6 m^3$)	ΣB_n ($10^6 m^3$)
1950	2000	1975	3,3	3,3	2537	243	2780	8,3	8,3	0,8	0,8	9,1	9,1
1900	1950	1925	12,7	16,0	2557	329	2886	32,5	40,8	4,2	5,0	36,7	45,8
1850	1900	1875	25,1	41,1	2446	262	2708	61,5	102,3	6,6	11,6	68,1	113,9
1800	1850	1825	14,8	55,9	2434	75	2509	36	138,3	1,1	12,7	37,1	151,0
1750	1800	1775	15,7	71,6	2396	-85	2311	37,5	175,8	-1,3	11,4	36,2	187,2
1700	1750	1725	28,1	99,7	2368	-189	2179	66,6	242,4	-5,3	6,0	61,2	248,4
1650	1700	1675	73,5	173,2	2328	-308	2020	171,1	413,5	-22,7	-16,6	148,4	396,8
1600	1650	1625	118,8	292,0	2297	-371	1925	272,9	686,4	-44,2	-60,8	228,8	625,6
1550	1600	1575	95,5	387,5	2238	-437	1801	213,9	900,3	-41,8	-102,6	172,1	797,7
1500	1550	1525	87,8	475,3	2129	-552	1577	187	1087,3	-48,5	-151,1	138,5	936,2
1450	1500	1475	73,7	549,0	1979	-691	1287	146	1233,3	-51,0	-202,1	95,0	1031,2
1400	1450	1425	61,2	610,2	1787	-851	935	109,4	1342,7	-52,1	-254,2	57,3	1088,4
1350	1400	1375	49,5	659,7	1563	-1066	496	77,3	1420	-52,8	-307,0	24,6	1113,0
1300	1350	1325	36,5	696,2	1356	-1315	41	49,6	1469,6	-48,1	-355,1	1,5	1114,5
1250	1300	1275	39,9	736,1	1161	-1603	-441	46,4	1515,9	-64,0	-419,0	-17,6	1096,9
1200	1250	1225	45,4	781,5	951	-2001	-1050	43,2	1559,2	-90,9	-509,9	-47,7	1049,2
1150	1200	1175	45,7	827,2	770	-2517	-1747	35,2	1594,3	-114,9	-624,9	-79,8	969,4
1100	1150	1125	43,0	870,2	690	-2993	-2302	29,7	1624,1	-128,9	-753,7	-99,1	870,3
1050	1100	1075	31,5	901,7	623	-3394	-2770	19,7	1643,7	-107,1	-860,8	-87,4	782,9
1000	1050	1025	33,0	934,7	553	-3749	-3196	18,2	1662	-123,7	-984,5	-105,4	677,5
950	1000	975	30,6	965,3	414	-4176	-3761	12,7	1674,6	-127,6	-1112,1	-114,9	562,6
900	950	925	25,7	991,0	246	-4649	-4403	6,3	1681	-119,5	-1231,6	-113,2	449,3
850	900	875	23,6	1014,6	114	-5074	-4959	2,7	1683,7	-119,9	-1351,5	-117,2	332,1
800	850	825	21,6	1036,2	30	-5429	-5398	0,7	1684,3	-117,1	-1468,6	-116,4	215,7
750	800	775	17,8	1054,0	-4	-5795	-5800	0	1684,3	-102,9	-1571,6	-103,0	112,7
700	750	725	5,4	1059,4	-7	-6076	-6083	0	1684,2	-32,6	-1604,1	-32,6	80,1

Brúarjökull

Elevation (m a.s.l.)			ΔS (km ²)	$\Sigma\Delta S$ (km ²)	b_w (mm)	b_s (mm)	b_n (mm)	ΔB_w (10 ⁶ m ³)	$\Sigma\Delta B_w$ (10 ⁶ m ³)	ΔB_s (10 ⁶ m ³)	$\Sigma\Delta B_s$ (10 ⁶ m ³)	ΔB_n (10 ⁶ m ³)	ΣB_n (10 ⁶ m ³)
1850	1900	1875	1,2	1,2	2799	-36	2762	3,3	3,4	0,0	0,0	3,3	3,4
1800	1850	1825	4,4	5,6	2799	24	2824	12,4	15,8	0,1	0,0	12,5	15,8
1750	1800	1775	2,9	8,5	2619	-64	2554	7,5	23,3	-0,2	-0,1	7,3	23,2
1700	1750	1725	3,9	12,4	2454	-160	2294	9,6	32,9	-0,6	-0,8	9,0	32,1
1650	1700	1675	5,5	17,9	2363	-271	2092	13	45,9	-1,5	-2,2	11,5	43,7
1600	1650	1625	50,9	68,8	2370	-461	1908	120,7	166,6	-23,5	-25,8	97,2	140,8
1550	1600	1575	46,0	114,8	2391	-519	1872	110	276,6	-23,9	-49,6	86,1	226,9
1500	1550	1525	72,6	187,4	2442	-532	1910	177,3	453,9	-38,7	-88,3	138,6	365,6
1450	1500	1475	78,3	265,7	2273	-578	1695	178	631,9	-45,3	-133,6	132,7	498,3
1400	1450	1425	111,2	376,9	2309	-667	1642	256,9	888,8	-74,2	-207,8	182,7	681,0
1350	1400	1375	155,9	532,8	2322	-842	1480	362	1250,8	-131,3	-339,1	230,8	911,7
1300	1350	1325	147,2	680,0	2249	-980	1269	331,1	1581,9	-144,3	-483,4	186,8	1098,5
1250	1300	1275	141,8	821,8	2137	-1058	1078	303,1	1885	-150,1	-633,5	152,9	1251,4
1200	1250	1225	117,9	939,7	1822	-1152	669	214,9	2099,9	-135,9	-769,5	79,0	1330,4
1150	1200	1175	102,7	1042,4	1526	-1358	168	156,8	2256,7	-139,5	-909,0	17,3	1347,6
1100	1150	1125	83,4	1125,8	1307	-1795	-488	109	2365,7	-149,8	-1058,8	-40,7	1306,9
1050	1100	1075	69,8	1195,6	1138	-2385	-1247	79,4	2445,1	-166,5	-1225,3	-87,1	1219,9
1000	1050	1025	62,5	1258,1	1001	-2915	-1913	62,6	2507,7	-182,1	-1407,4	-119,5	1100,3
950	1000	975	56,4	1314,5	905	-3427	-2522	51,1	2558,8	-193,4	-1600,8	-142,3	958,0
900	950	925	46,3	1360,8	817	-3898	-3080	37,9	2596,7	-180,5	-1781,3	-142,6	815,4
850	900	875	42,6	1403,4	713	-4326	-3613	30,4	2627	-184,1	-1965,4	-153,8	661,6
800	850	825	38,1	1441,5	597	-4687	-4090	22,8	2649,8	-178,7	-2144,1	-155,9	505,7
750	800	775	37,0	1478,5	435	-5031	-4596	16,1	2665,9	-186,3	-2330,4	-170,2	335,5
700	750	725	25,6	1504,1	332	-5363	-5031	8,5	2674,4	-137,4	-2467,8	-128,9	206,6
650	700	675	17,5	1521,6	252	-5697	-5445	4,4	2678,8	-99,4	-2567,2	-95,0	111,6
600	650	625	3,0	1524,6	211	-6024	-5813	0,6	2679,5	-18,1	-2585,3	-17,4	94,2

Eyjabakkajökull

Elevation (m a.s.l.)			ΔS (km ²)	$\Sigma\Delta S$ (km ²)	b_w (mm)	b_s (mm)	b_n (mm)	ΔB_w (10 ⁶ m ³)	$\Sigma\Delta B_w$ (10 ⁶ m ³)	ΔB_s (10 ⁶ m ³)	$\Sigma\Delta B_s$ (10 ⁶ m ³)	ΔB_n (10 ⁶ m ³)	ΣB_n (10 ⁶ m ³)
1550	1600	1575	0,0	0,0	3435	-982	2452	0	0	0,0	0,0	0,0	0,0
1500	1550	1525	0,0	0,0	3443	-974	2469	0,3	0,3	0,0	0,0	0,2	0,2
1450	1500	1475	1,0	1,0	3424	-987	2436	3,3	3,7	-1,0	-1,1	2,4	2,6
1400	1450	1425	1,8	2,8	3383	-1003	2379	6,3	9,9	-1,9	-2,9	4,4	7,0
1350	1400	1375	2,5	5,3	3269	-1040	2229	8,3	18,2	-2,6	-5,5	5,6	12,7
1300	1350	1325	4,1	9,4	3146	-1079	2067	13	31,2	-4,4	-10,0	8,5	21,2
1250	1300	1275	13,7	23,1	2809	-1015	1794	38,5	69,7	-13,9	-23,9	24,6	45,8
1200	1250	1225	13,4	36,5	2606	-1252	1353	34,9	104,6	-16,8	-40,7	18,1	63,9
1150	1200	1175	14,4	50,9	2390	-1542	848	34,4	139	-22,2	-62,9	12,2	76,1
1100	1150	1125	12,1	63,0	2152	-1979	173	26,1	165,1	-24,0	-86,9	2,1	78,2
1050	1100	1075	10,4	73,4	1888	-2650	-761	19,6	184,7	-27,5	-114,4	-7,9	70,3
1000	1050	1025	10,1	83,5	1642	-3246	-1603	16,6	201,3	-32,8	-147,2	-16,2	54,1
950	1000	975	7,6	91,1	1399	-3735	-2336	10,6	211,9	-28,2	-175,4	-17,7	36,5
900	950	925	4,9	96,0	1226	-4182	-2956	6,1	217,9	-20,7	-196,1	-14,6	21,9
850	900	875	4,0	100,0	1145	-4452	-3306	4,5	222,4	-17,6	-213,7	-13,1	8,8
800	850	825	3,1	103,1	1094	-4664	-3570	3,3	225,8	-14,3	-228,0	-10,9	-2,2
750	800	775	3,0	106,1	1008	-5071	-4063	3,1	228,9	-15,4	-243,4	-12,4	-14,5
700	750	725	2,6	108,7	883	-5623	-4739	2,3	231,2	-14,7	-258,1	-12,4	-26,9
650	700	675	3,0	111,7	757	-5995	-5237	2,3	233,5	-18,3	-276,3	-16,0	-42,9
600	650	625	0,2	111,9	657	-6128	-5471	0,1	233,6	-1,0	-277,3	-0,9	-43,7

Hoffellsjökull

Elevation (m a.s.l.)			ΔS (km ²)	$\Sigma \Delta S$ (km ²)	b_w (mm)	b_s (mm)	b_n (mm)	ΔB_w (10 ⁶ m ³)	$\Sigma \Delta B_w$ (10 ⁶ m ³)	ΔB_s (10 ⁶ m ³)	$\Sigma \Delta B_s$ (10 ⁶ m ³)	ΔB_n (10 ⁶ m ³)	ΣB_n (10 ⁶ m ³)
1450	1500	1475	0,9	0,9	3433	-982	2450	3,2	3,2	-0,9	-0,9	2,3	2,3
1400	1450	1425	6,7	7,6	3178	-854	2323	23	26,1	-6,2	-7,1	16,8	19,1
1350	1400	1375	10,0	17,6	3165	-904	2261	32,2	58,4	-9,2	-16,3	23,0	42,1
1300	1350	1325	15,4	33,0	3099	-978	2120	50,5	108,9	-15,9	-32,2	34,5	76,6
1250	1300	1275	33,6	66,6	2933	-1017	1915	102,5	211,3	-35,6	-67,8	66,9	143,5
1200	1250	1225	26,8	93,4	2869	-1150	1719	74,1	285,5	-29,7	-97,5	44,4	187,9
1150	1200	1175	18,2	111,6	2708	-1305	1403	48,6	334,1	-23,4	-120,9	25,2	213,1
1100	1150	1125	17,5	129,1	2450	-1472	977	41,5	375,6	-24,9	-145,9	16,6	229,7
1050	1100	1075	13,6	142,7	2067	-1675	391	26,4	402	-21,4	-167,3	5,0	234,7
1000	1050	1025	10,0	152,7	1748	-1862	-113	17	419,1	-18,2	-185,5	-1,1	233,6
950	1000	975	9,0	161,7	1485	-2019	-534	12,9	431,9	-17,5	-203,0	-4,6	229,0
900	950	925	6,4	168,1	1283	-2172	-888	8,2	440,2	-13,9	-216,9	-5,7	223,3
850	900	875	4,3	172,4	1163	-2297	-1134	5	445,2	-10,0	-226,9	-4,9	218,3
800	850	825	3,6	176,0	1080	-2409	-1329	3,8	449	-8,6	-235,4	-4,7	213,6
750	800	775	3,9	179,9	962	-2517	-1554	3,7	452,8	-9,7	-245,2	-6,0	207,6
700	750	725	3,8	183,7	838	-2603	-1764	3	455,8	-9,4	-254,6	-6,4	201,2
650	700	675	3,4	187,1	674	-2711	-2036	2,3	458,1	-9,4	-263,9	-7,0	194,2
600	650	625	2,5	189,6	461	-2836	-2375	1,2	459,3	-7,2	-271,1	-6,0	188,2
550	600	575	1,8	191,4	290	-2986	-2696	0,5	459,8	-5,1	-276,3	-4,6	183,5
500	550	525	1,5	192,9	190	-3205	-3015	0,3	460,1	-5,1	-281,4	-4,8	178,8
450	500	475	0,9	193,8	111	-3467	-3356	0	460,2	-3,1	-284,4	-3,0	175,8
400	450	425	0,9	194,7	33	-3777	-3743	0	460,2	-3,6	-288,0	-3,5	172,3
350	400	375	0,6	195,3	-51	-4188	-4240	0	460,2	-2,7	-290,6	-2,7	169,6
300	350	325	0,9	196,2	-139	-4649	-4788	-0,1	460,1	-3,3	-294,0	-3,4	166,1
250	300	275	2,2	198,4	-232	-5146	-5379	-0,3	459,8	-6,7	-300,7	-7,0	159,1
200	250	225	3,3	201,7	-331	-5694	-6026	-0,9	458,9	-15,2	-315,9	-16,1	143,0
150	200	175	2,6	204,3	-457	-6246	-6704	-1,4	457,5	-18,7	-334,6	-20,0	122,9
100	150	125	2,1	206,4	-578	-6628	-7207	-1,4	456,2	-15,6	-350,2	-17,0	105,9
50	100	75	2,8	209,2	-656	-6896	-7553	-1,2	455	-12,8	-363,0	-14,0	92,0
0	50	25	0,6	209,8	-741	-7297	-8039	-1,9	453	-19,1	-382,1	-21,1	70,9

Breiðamerkurjökull

Elevation (m a.s.l.)			ΔS (km ²)	$\Sigma \Delta S$ (km ²)	b_w (mm)	b_s (mm)	b_n (mm)	ΔB_w (10 ⁶ m ³)	$\Sigma \Delta B_w$ (10 ⁶ m ³)	ΔB_s (10 ⁶ m ³)	$\Sigma \Delta B_s$ (10 ⁶ m ³)	ΔB_n (10 ⁶ m ³)	ΣB_n (10 ⁶ m ³)
1900	1950	1925	0,0	0,0	4329	256	4586	0,3	0,3	0,0	0,0	0,4	0,4
1850	1900	1875	0,4	0,4	4339	189	4528	1,6	2	0,0	0,0	1,7	2,0
1800	1850	1825	0,4	0,8	4360	78	4438	2	4	0,0	0,1	2,1	4,1
1750	1800	1775	0,8	1,6	4365	-43	4321	4,4	8,4	0,0	0,0	4,3	8,5
1700	1750	1725	2,5	4,1	3650	-104	3546	9,6	17,9	-0,3	-0,2	9,3	17,7
1650	1700	1675	5,8	9,9	3056	-173	2883	18,3	36,2	-1,0	-1,2	17,3	35,0
1600	1650	1625	15,8	25,7	2899	-329	2569	49,7	86	-5,7	-6,9	44,1	79,1
1550	1600	1575	25,7	51,4	2776	-421	2354	72,1	158	-10,9	-17,8	61,1	140,2
1500	1550	1525	32,2	83,6	2678	-507	2171	85,6	243,7	-16,2	-34,1	69,4	209,6
1450	1500	1475	44,3	127,9	2630	-605	2025	120,9	364,5	-27,8	-61,9	93,1	302,7
1400	1450	1425	58,3	186,2	2552	-757	1794	151,2	515,7	-44,9	-106,7	106,3	409,0
1350	1400	1375	88,7	274,9	2538	-985	1552	227	742,8	-88,1	-194,9	138,9	547,9
1300	1350	1325	96,9	371,8	2565	-1149	1415	244,1	986,9	-109,4	-304,3	134,7	682,6
1250	1300	1275	59,4	431,2	2539	-1272	1267	146,2	1133,1	-73,3	-377,6	73,0	755,6
1200	1250	1225	39,7	470,9	2436	-1369	1067	96,8	1230	-54,4	-432,0	42,4	798,0
1150	1200	1175	32,6	503,5	2293	-1469	824	72,8	1302,8	-46,6	-478,6	26,2	824,2
1100	1150	1125	27,7	531,2	2143	-1587	555	58,5	1361,2	-43,3	-521,9	15,2	839,3
1050	1100	1075	24,1	555,3	1992	-1704	287	47,4	1408,6	-40,6	-562,5	6,8	846,2
1000	1050	1025	22,1	577,4	1862	-1810	51	40,7	1449,4	-39,6	-602,1	1,1	847,3
950	1000	975	24,5	601,9	1742	-1903	-160	42,4	1491,8	-46,3	-648,4	-3,9	843,4
900	950	925	27,4	629,3	1639	-1994	-354	44,4	1536,2	-54,0	-702,4	-9,6	833,8
850	900	875	26,2	655,5	1417	-2172	-755	36,1	1572,3	-55,3	-757,8	-19,2	814,6
800	850	825	26,1	681,6	1178	-2377	-1199	30,4	1602,7	-61,3	-819,0	-30,9	783,7
750	800	775	25,3	706,9	938	-2641	-1702	23,6	1626,3	-66,5	-885,5	-42,8	740,8
700	750	725	23,9	730,8	792	-2847	-2055	17,6	1643,9	-63,3	-948,7	-45,7	695,1
650	700	675	30,8	761,6	693	-3027	-2333	21,8	1665,7	-95,0	-1043,7	-73,2	621,9
600	650	625	26,2	787,8	496	-3268	-2772	12,7	1678,4	-83,8	-1127,6	-71,1	550,8
550	600	575	27,0	814,8	297	-3553	-3255	8	1686,4	-95,6	-1223,2	-87,6	463,2
500	550	525	15,7	830,5	236	-3609	-3373	3,7	1690,1	-56,2	-1279,4	-52,5	410,7
450	500	475	16,3	846,8	78	-3791	-3713	1,1	1691,2	-55,2	-1334,6	-54,1	356,6
400	450	425	15,9	862,7	27	-3922	-3894	0,5	1691,7	-64,6	-1399,2	-64,1	292,5
350	400	375	13,0	875,7	-41	-4183	-4225	-0,5	1691,1	-55,1	-1454,3	-55,7	236,8
300	350	325	13,1	888,8	-124	-4617	-4742	-1,4	1689,7	-53,6	-1507,9	-55,0	181,8
250	300	275	12,1	900,9	-220	-5144	-5365	-2,5	1687,2	-57,4	-1565,3	-59,9	121,9
200	250	225	11,5	912,4	-327	-5706	-6033	-3,7	1683,5	-65,2	-1630,5	-68,9	53,0
150	200	175	8,6	921,0	-459	-6281	-6741	-4,3	1679,2	-58,9	-1689,4	-63,2	-10,2
100	150	125	7,9	928,9	-587	-6768	-7355	-4,7	1674,5	-54,0	-1743,4	-58,7	-68,9
50	100	75	6,1	935,0	-681	-7128	-7810	-5	1669,5	-52,5	-1795,9	-57,5	-126,4
0	50	25	3,0	938,0	-740	-7357	-8098	-4,1	1665,3	-41,1	-1837,0	-45,3	-171,7

Síðujökull

Elevation (m a.s.l.)			ΔS (km ²)	$\Sigma \Delta S$ (km ²)	b_w (mm)	b_s (mm)	b_n (mm)	ΔB_w (10 ⁶ m ³)	$\Sigma \Delta B_w$ (10 ⁶ m ³)	ΔB_s (10 ⁶ m ³)	$\Sigma \Delta B_s$ (10 ⁶ m ³)	ΔB_n (10 ⁶ m ³)	ΣB_n (10 ⁶ m ³)
1700	1750	1725	0,8	0,8	3047	-19	3027	2,6	2,6	0,0	0,0	2,5	2,5
1650	1700	1675	5,5	6,3	2896	-286	2609	16	18,6	-1,6	-1,6	14,5	17,0
1600	1650	1625	11,1	17,4	2750	-396	2354	30,5	49,1	-4,4	-6,0	26,1	43,1
1550	1600	1575	10,7	28,1	2684	-413	2271	28,8	77,9	-4,4	-10,4	24,4	67,5
1500	1550	1525	20,5	48,6	2608	-487	2121	53,3	131,3	-10,0	-20,4	43,4	110,9
1450	1500	1475	39,0	87,6	2437	-674	1762	95,2	226,4	-26,3	-46,7	68,8	179,7
1400	1450	1425	25,9	113,5	2319	-835	1484	60,1	286,5	-21,6	-68,4	38,5	218,2
1350	1400	1375	21,2	134,7	2253	-990	1262	47,7	334,2	-21,0	-89,4	26,7	244,9
1300	1350	1325	17,3	152,0	2203	-1109	1093	38,2	372,4	-19,2	-108,6	18,9	263,8
1250	1300	1275	15,9	167,9	2159	-1228	931	34,4	406,8	-19,6	-128,1	14,8	278,7
1200	1250	1225	21,1	189,0	2150	-1331	818	45,4	452,2	-28,1	-156,3	17,3	296,0
1150	1200	1175	18,3	207,3	2110	-1509	601	38,5	490,8	-27,5	-183,8	11,0	306,9
1100	1150	1125	17,2	224,5	2124	-1771	352	36,6	527,4	-30,5	-214,3	6,1	313,0
1050	1100	1075	16,2	240,7	2124	-2047	77	34,5	561,8	-33,2	-247,6	1,3	314,3
1000	1050	1025	20,5	261,2	2057	-2374	-317	42,2	604	-48,7	-296,3	-6,5	307,7
950	1000	975	20,2	281,4	1855	-2751	-896	37,4	641,4	-55,5	-351,8	-18,1	289,7
900	950	925	21,6	303,0	1584	-3060	-1475	34,3	675,7	-66,2	-418,0	-31,9	257,8
850	900	875	19,8	322,8	1400	-3292	-1891	27,7	703,4	-65,1	-483,1	-37,4	220,3
800	850	825	21,3	344,1	1258	-3486	-2228	26,7	730,2	-74,1	-557,2	-47,3	173,0
750	800	775	23,3	367,4	1103	-3649	-2545	25,8	755,9	-85,2	-642,4	-59,4	113,6
700	750	725	23,6	391,0	913	-3841	-2927	21,6	777,5	-90,6	-733,0	-69,1	44,5
650	700	675	19,9	410,9	711	-4061	-3349	14,1	791,6	-80,6	-813,6	-66,5	-22,0
600	650	625	10,9	421,8	575	-4189	-3613	6,3	797,9	-45,7	-859,3	-39,4	-61,4
550	600	575	1,5	423,3	511	-4234	-3723	0,8	798,7	-6,5	-865,8	-5,7	-67,1

Skaftárjökull

Elevation (m a.s.l.)			ΔS (km ²)	$\Sigma \Delta S$ (km ²)	b_w (mm)	b_s (mm)	b_n (mm)	ΔB_w (10 ⁶ m ³)	$\Sigma \Delta B_w$ (10 ⁶ m ³)	ΔB_s (10 ⁶ m ³)	$\Sigma \Delta B_s$ (10 ⁶ m ³)	ΔB_n (10 ⁶ m ³)	ΣB_n (10 ⁶ m ³)
1350	1400	1375	2,3	2,3	2100	-1004	1096	4,9	4,9	-2,4	-2,4	2,6	2,6
1300	1350	1325	5,4	7,7	2051	-1126	925	11	15,9	-6,0	-8,4	4,9	7,5
1250	1300	1275	4,2	11,9	2032	-1265	767	8,6	24,5	-5,4	-13,7	3,3	10,8
1200	1250	1225	6,5	18,4	2009	-1424	584	13	37,5	-9,2	-23,0	3,8	14,5
1150	1200	1175	7,9	26,3	1965	-1618	347	15,5	53	-12,8	-35,7	2,7	17,3
1100	1150	1125	11,2	37,5	1896	-1869	26	21,1	74,2	-20,8	-56,6	0,3	17,6
1050	1100	1075	12,9	50,4	1802	-2182	-380	23,3	97,4	-28,2	-84,8	-4,9	12,7
1000	1050	1025	12,9	63,3	1685	-2530	-844	21,8	119,3	-32,7	-117,5	-10,9	1,7
950	1000	975	8,5	71,8	1520	-2935	-1415	13	132,2	-25,0	-142,5	-12,1	-10,3
900	950	925	5,5	77,3	1397	-3266	-1869	7,6	139,9	-17,9	-160,4	-10,2	-20,5
850	900	875	5,3	82,6	1275	-3616	-2340	6,8	146,7	-19,3	-179,7	-12,5	-33,0
800	850	825	5,0	87,6	1148	-3991	-2843	5,7	152,4	-19,9	-199,6	-14,2	-47,2
750	800	775	4,8	92,4	1018	-4337	-3319	4,9	157,3	-20,9	-220,5	-16,0	-63,2
700	750	725	4,4	96,8	848	-4698	-3850	3,7	161,1	-20,8	-241,3	-17,0	-80,2
650	700	675	2,6	99,4	698	-4951	-4252	1,8	162,9	-12,8	-254,1	-11,0	-91,2
600	650	625	0,7	100,1	553	-5111	-4557	0,4	163,2	-3,4	-257,4	-3,0	-94,2

Vestari Skaftárketill

Elevation (m a.s.l.)			ΔS (km ²)	$\Sigma \Delta S$ (km ²)	b_w (mm)	b_s (mm)	b_n (mm)	ΔB_w (10 ⁶ m ³)	$\Sigma \Delta B_w$ (10 ⁶ m ³)	ΔB_s (10 ⁶ m ³)	$\Sigma \Delta B_s$ (10 ⁶ m ³)	ΔB_n (10 ⁶ m ³)	ΣB_n (10 ⁶ m ³)
1900	1950	1925	0,6	0,6	2456	194	2651	1,4	1,4	0,1	0,1	1,5	1,5
1850	1900	1875	0,6	1,2	2435	132	2568	1,5	2,9	0,0	0,2	1,6	3,1
1800	1850	1825	0,8	2,0	2409	52	2461	1,9	4,7	0,0	0,2	1,9	5,0
1750	1800	1775	2,6	4,6	2330	-129	2200	6	10,8	-0,3	-0,1	5,7	10,7
1700	1750	1725	5,5	10,1	2183	-239	1943	12,1	22,8	-1,3	-1,4	10,7	21,4
1650	1700	1675	6,6	16,7	2032	-310	1721	13,5	36,3	-2,1	-3,5	11,4	32,8
1600	1650	1625	7,6	24,3	1973	-369	1603	15	51,3	-2,8	-6,3	12,2	45,0
1550	1600	1575	5,5	29,8	1925	-437	1488	10,5	61,8	-2,4	-8,7	8,1	53,1
1500	1550	1525	1,5	31,3	1909	-469	1440	2,9	64,7	-0,7	-9,4	2,2	55,3

Eystri Skaftárketill

Elevation (m a.s.l.)			ΔS (km ²)	$\Sigma \Delta S$ (km ²)	b_w (mm)	b_s (mm)	b_n (mm)	ΔB_w (10 ⁶ m ³)	$\Sigma \Delta B_w$ (10 ⁶ m ³)	ΔB_s (10 ⁶ m ³)	$\Sigma \Delta B_s$ (10 ⁶ m ³)	ΔB_n (10 ⁶ m ³)	ΣB_n (10 ⁶ m ³)
1750	1800	1775	1,1	1,1	2316	-211	2104	2,5	2,5	-0,2	-0,2	2,3	2,3
1700	1750	1725	10,2	11,3	2209	-334	1874	22,5	25	-3,4	-3,6	19,1	21,4
1650	1700	1675	16,5	27,8	2155	-427	1728	35,6	60,6	-7,1	-10,7	28,6	49,9
1600	1650	1625	9,7	37,5	2089	-404	1685	20,2	80,8	-3,9	-14,6	16,3	66,2
1550	1600	1575	2,4	39,9	2079	-400	1679	5,1	85,9	-1,0	-15,6	4,1	70,3

Gjálp

Elevation (m a.s.l.)			ΔS (km ²)	$\Sigma \Delta S$ (km ²)	b_w (mm)	b_s (mm)	b_n (mm)	ΔB_w (10 ⁶ m ³)	$\Sigma \Delta B_w$ (10 ⁶ m ³)	ΔB_s (10 ⁶ m ³)	$\Sigma \Delta B_s$ (10 ⁶ m ³)	ΔB_n (10 ⁶ m ³)	ΣB_n (10 ⁶ m ³)
1900	1950	1925	0,4	0,4	2462	220	2682	0,9	0,9	0,0	0,0	1,0	1,0
1850	1900	1875	0,7	1,1	2431	122	2554	1,8	2,7	0,0	0,2	1,9	2,9
1800	1850	1825	1,1	2,2	2399	5	2405	2,7	5,4	0,0	0,2	2,7	5,6
1750	1800	1775	4,9	7,1	2340	-213	2127	11,4	16,8	-1,0	-0,9	10,3	16,0
1700	1750	1725	18,8	25,9	2286	-381	1904	42,9	59,7	-7,2	-8,0	35,7	51,7
1650	1700	1675	13,5	39,4	2290	-454	1835	30,9	90,6	-6,1	-14,2	24,8	76,5

Grímsvötn

Elevation (m a.s.l.)			ΔS (km ²)	$\Sigma \Delta S$ (km ²)	b_w (mm)	b_s (mm)	b_n (mm)	ΔB_w (10 ⁶ m ³)	$\Sigma \Delta B_w$ (10 ⁶ m ³)	ΔB_s (10 ⁶ m ³)	$\Sigma \Delta B_s$ (10 ⁶ m ³)	ΔB_n (10 ⁶ m ³)	ΣB_n (10 ⁶ m ³)
1700	1750	1725	0,7	0,7	2327	-433	1893	1,7	1,7	-0,3	-0,3	1,4	1,4
1650	1700	1675	40,6	41,3	2355	-489	1866	95,6	97,4	-19,9	-20,2	75,8	77,2
1600	1650	1625	30,8	72,1	2394	-645	1749	73,8	171,1	-19,9	-40,1	53,9	131,1
1550	1600	1575	19,2	91,3	2363	-868	1495	45,4	216,5	-16,7	-56,7	28,7	159,8
1500	1550	1525	16,9	108,2	2349	-1125	1223	39,8	256,3	-19,0	-75,8	20,7	180,5
1450	1500	1475	10,0	118,2	2388	-1280	1107	24	280,3	-12,8	-88,6	11,1	191,6
1400	1450	1425	11,7	129,9	2440	-1344	1095	28,5	308,8	-15,7	-104,4	12,8	204,4
1350	1400	1375	4,3	134,2	2497	-1352	1144	10,8	319,6	-5,9	-110,2	5,0	209,4
1300	1350	1325	0,7	134,9	2627	-1299	1328	2	321,6	-1,0	-111,2	1,0	210,4

Appendix C: Coordinates at velocity measurement stakes in 2018.

Position of velocity measurement stakes determined by GPS sub-metre differential (I), fast static (FS) and kinematic (K). (Accuracy of horizontal position 0.5 – 1.0 m, and vertical accuracy 1-2 m for DGPS, about 1cm for fast static, and 3 cm for kinematic).

The station Hofn in Höfn í Hornafirði is used as a stationary reference for all measurements, ÍSN93 datum, h_1 is elevation above ellipsoid, dL antenna height, N estimated difference between ellipsoid and sea-level, H elevation in metres above sea level ($H=h_1+N+dL$). X and Y are ÍSN93 Lambert conformal conic projected coordinates. M is a quality marker.

Site	time	Calender				Latitude	Longitude	h_1 (m a. e.)	dL (m)	N (m)	H (m a. s. l.)	X	Y	M		
		Date	#	Year	Day											
B07-18	12,791	9	5	129	2018	64	25,7946	16	17,4554	1427,1	0	-67,1	1360,1	630474,7	439242,2	K
B07-18	12,048	9	10	282	2018	64	25,7938	16	17,4539	1423,2	0	-67,1	1356,2	630476	439240,7	K
B09-18	11,347	10	5	130	2018	64	45,0399	16	5,46403	792,56	0	-66,7	725,9	638448,9	475389,6	K
B09-18	19,179	9	10	282	2018	64	45,0397	16	5,46311	786,85	0	-66,7	720,18	638449,6	475389,3	K
B10-18	12,546	10	5	130	2018	64	43,6858	16	6,69983	851,97	0	-66,7	785,26	637584,2	472831,4	K
B10-18	19,814	9	10	282	2018	64	43,6854	16	6,70097	846,2	0	-66,7	779,49	637583,3	472830,6	K
B11-18	10,655	10	5	130	2018	64	40,9692	16	10,4661	1019,5	0	-66,8	952,64	634821,7	467653,9	K
B11-18	18,369	9	10	282	2018	64	40,9732	16	10,4626	1015,5	0	-66,8	948,64	634824,1	467661,4	K
B12-18	9,771	10	5	130	2018	64	38,2671	16	14,1298	1144,8	0	-66,9	1077,9	632129,5	462509,3	K
B12-18	18,003	9	10	282	2018	64	38,276	16	14,1217	1141,3	0	-66,9	1074,4	632135,2	462526,2	K
B13-18	14,264	10	5	130	2018	64	34,5365	16	19,6957	1286,6	0	-67	1219,5	627991,3	455393,5	K
B13-18	17,461	9	10	282	2018	64	34,5469	16	19,6837	1283,3	0	-67	1216,2	628000	455413,2	K
B13ror15	19,44	9	5	129	2018	64	34,573	16	19,6748	1285	0	-67	1218	628005,1	455461,9	K
B13ror15	17,565	9	10	282	2018	64	34,5833	16	19,662	1282,2	2,62	-67	1217,8	628014,5	455481,5	K
B14-18	18,603	9	5	129	2018	64	31,6343	16	24,7077	1388,6	0	-67,1	1321,4	624212,5	449839,2	K
B14-18	17,948	9	10	282	2018	64	31,6425	16	24,6928	1385,5	0	-67,1	1318,4	624223,9	449855	K
B15-18	17,922	9	5	129	2018	64	28,4887	16	30,0196	1472,3	0	-67,2	1405,1	620197,1	443828,3	K
B15-18	16,525	9	10	282	2018	64	28,4933	16	30,0078	1468,6	0	-67,2	1401,4	620206,2	443837,2	K
B16-18	17,441	9	5	129	2018	64	24,1272	16	40,8604	1597,7	0	-67,3	1530,3	611810,3	435399	K
B16-18	12,704	9	10	282	2018	64	24,1274	16	40,8598	1593,5	0	-67,3	1526,2	611810,8	435399,4	K
B17-18	8,957	10	5	130	2018	64	36,7357	16	28,7997	1283	0	-67,1	1215,9	620563,6	459177,8	K
B17-18	17,118	9	10	282	2018	64	36,7467	16	28,7915	1280,7	0	-67,1	1213,6	620569,3	459198,5	K
B18-18	21,133	8	5	128	2018	64	31,5839	16	0,12555	1382,7	0	-66,9	1315,8	643865,6	450614,4	K
B18-18	17,321	9	10	282	2018	64	31,5889	16	0,12892	1378,9	0	-66,9	1312	643862,5	450623,5	K
B19-18	20,875	8	5	128	2018	64	27,9963	15	55,9807	1508	0	-66,9	1441,1	647501,4	444115,5	K
B19-18	12,287	9	10	282	2018	64	27,9965	15	55,9813	1503,4	0	-66,9	1436,5	647500,9	444115,8	K
BB0-18	18,546	8	5	128	2018	64	22,7072	16	5,04878	1588,6	0	-66,9	1521,7	640691,3	433954,8	K
BB0-18	18,364	8	10	281	2018	64	22,707	16	5,04978	1583,9	0	-66,9	1517,1	640690,5	433954,5	K
BB08-18	0,341	8	6	159	2018	64	37,1914	17	29,5119	1985,8	0	-67,9	1918	572145,1	458481,8	K
BB09-18	0,509	8	6	159	2018	64	36,5192	17	30,5536	1981,8	0	-67,9	1913,9	571344,3	457213,6	K
BB11-18	0,716	8	6	159	2018	64	36,0449	17	31,4215	1959,3	0	-67,9	1891,4	570672,7	456316,3	K
BB15-18	0,157	8	6	159	2018	64	38,1017	17	30,6189	2000,6	0	-67,9	1932,8	571222,9	460151,7	K
BB17-18	23,907	7	6	158	2018	64	38,5842	17	28,8607	1983,7	0	-67,9	1915,8	572602,1	461081,4	K
BB18-18	23,689	7	6	158	2018	64	39,5206	17	26,6825	1965,7	0	-67,9	1897,9	574294,1	462862,8	K
BB19-18	23,434	7	6	158	2018	64	39,11	17	22,9131	1932,1	0	-67,8	1864,3	577313,9	462175,4	K
BB20-18	23,211	7	6	158	2018	64	38,9701	17	23,4907	1941,6	0	-67,9	1873,7	576860,7	461903,8	K
BB21-18	22,969	7	6	158	2018	64	38,6742	17	24,7986	1939,5	0	-67,9	1871,6	575833,1	461328	K
BB22-18	22,679	7	6	158	2018	64	38,4339	17	25,621	1946,6	0	-67,9	1878,7	575189,3	460865,2	K
BB23-18	1,061	8	6	159	2018	64	37,136	17	27,5243	1971,6	0	-67,9	1903,8	573732,1	458417,1	K
BB24-18	22,212	7	6	158	2018	64	37,1932	17	24,5721	1939,9	0	-67,9	1872	576082,7	458581,7	K
BB31-18	13,036	8	6	159	2018	64	42,0491	17	15,1923	1529,9	0	-67,6	1462,3	583310	467797,9	K
BB35-18	13,328	8	6	159	2018	64	40,9864	17	18,1763	1607,4	0	-67,7	1539,7	580991,6	465759,5	K
BB36-18	13,621	8	6	159	2018	64	40,1305	17	20,263	1719,4	0	-67,8	1651,7	579374	464125,7	K
BB42-18	16,418	8	6	159	2018	64	35,5432	17	31,7573	1921	0	-67,9	1853,2	570426,5	455378,2	K
BB43-18	15,786	8	6	159	2018	64	34,9479	17	32,826	1826,1	0	-67,9	1758,3	569599,2	454252,6	K
BB44-18	16,778	8	6	159	2018	64	34,1435	17	35,9046	1747,6	0	-67,8	1679,8	567174,7	452703	K
BB46-18	17,161	8	6	159	2018	64	33,5408	17	36,5906	1728,6	0	-67,8	1660,8	566651,5	451571,3	K
NV91-18	12,147	8	6	159	2018	64	35,0636	17	20,4188	1787,7	0	-67,8	1719,9	579497,2	454711,4	K

K04-18	15,025	10	10	283	2018	64	33,2126	17	42,2659	1553,6	0	-67,7	1485,8	562129,6	450865,3	K
K05-18	20,029	11	5	131	2018	64	33,4454	17	35,4301	1750,2	0	-67,8	1682,3	567582,6	451414,7	K
K05-18	14,558	10	10	283	2018	64	33,4427	17	35,4437	1747,1	0	-67,8	1679,2	567571,9	451409,3	K
K06-18	15,605	5	6	156	2018	64	38,3514	17	31,3565	2015,7	0	-67,9	1947,8	570624,4	460601,8	K
K06-18	13,294	10	10	283	2018	64	38,3505	17	31,3538	2013,6	0	-67,9	1945,7	570626,6	460600,1	K
K07-18	9,654	12	5	132	2018	64	29,1151	17	42,0433	1602,3	0	-67,7	1534,6	562464	443257,3	K
K07-18	16,354	10	10	283	2018	64	29,1151	17	42,0447	1599,2	0	-67,7	1531,5	562462,8	443257,4	K
Or07-18	20,417	3	6	154	2018	64	0,41913	16	39,0407	1921,1	-1,55	-66,4	1853,1	614908,6	391433	K
S01-18	16,218	12	5	132	2018	64	7,00173	17	49,9668	790,9	0	-66,8	724,06	556874,5	402053,6	K
S01-18	14,989	10	10	283	2018	64	7,00198	17	49,9663	786,81	0	-66,8	719,97	556874,8	402054,1	K
S02-18	15,472	12	5	132	2018	64	12,159	17	48,9649	1073,4	0	-67,1	1006,4	557508,5	411649,4	K
S02-18	14,304	10	10	283	2018	64	12,1508	17	48,9682	1068,7	0	-67	1001,6	557506,2	411634,1	K
S04-18	14,943	12	5	132	2018	64	16,1863	17	48,1924	1228	0	-67,2	1160,8	557992,2	419142,6	K
S04-18	13,334	10	10	283	2018	64	16,1759	17	48,2034	1224,2	0	-67,2	1157	557983,7	419123,1	K
S05-18	13,937	12	5	132	2018	64	20,4982	17	33,998	1520,5	0	-67,5	1453	569272,2	427390,7	K
S05-18	12,046	10	10	283	2018	64	20,4966	17	34,0115	1516,5	0	-67,5	1449	569261,5	427387,4	K
Ske02-18	12,996	13	5	133	2018	64	18,1607	17	9,17887	1276,2	0	-67,2	1209	589385,2	423568	K
Ske02-18	14,203	9	10	282	2018	64	18,1488	17	9,20446	1270,9	0	-67,2	1203,7	589365,2	423545,4	K
Ske03-18	15,427	9	5	129	2018	64	17,8006	17	0,00363	1321,9	0	-67,2	1254,7	596804,5	423124,6	K
Ske04-18	14,718	9	5	129	2018	64	19,4922	16	54,5136	1435,6	0	-67,3	1368,4	601127,9	426409,1	K
Ske04-18	13,284	9	10	282	2018	64	19,4752	16	54,5567	1431,2	0	-67,3	1364	601094,2	426376,4	K
Ske05-18	14,029	9	5	129	2018	64	21,7044	16	51,0166	1504,1	0	-67,3	1436,8	603805,3	430611,5	K
Ske05-18	13,033	9	10	282	2018	64	21,6942	16	51,0297	1499,8	0	-67,3	1432,5	603795,4	430592,3	K
Skf00-18	19,361	7	5	127	2018	64	15,4602	15	54,0642	1018,2	0	-66	952,21	650177,7	420926,3	K
Skf00-18	15,693	8	10	281	2018	64	15,4613	15	54,0617	1014,1	0	-66	948,06	650179,6	420928,4	K
Skf01-18	14,787	8	5	128	2018	64	17,9858	16	5,00803	1352,5	0	-66,6	1285,9	641128,6	425193,3	K
Skf01-18	17,164	8	10	281	2018	64	17,9836	16	4,99434	1347,2	0	-66,6	1280,6	641139,8	425189,7	K
T01ve-18	16,864	12	5	132	2018	64	19,545	18	7,07716	845,49	0	-67,3	778,23	542654,9	425131,8	K
T01ve-18	18,704	10	10	283	2018	64	19,5444	18	7,07671	839,17	0	-67,3	771,91	542655,3	425130,6	K
T02-18	15,021	12	5	132	2018	64	19,5984	18	4,01718	994,41	0	-67,3	927,14	545119,5	425266,4	K
T02-18	18,302	10	10	283	2018	64	19,5987	18	4,02193	989,49	0	-67,3	922,22	545115,7	425266,9	K
T03-18	18,572	12	5	132	2018	64	20,2055	17	58,5913	1139,3	0	-67,3	1072	549473,9	426461,9	K
T03-18	16,6	10	10	283	2018	64	20,2038	17	58,6001	1135,9	0	-67,3	1068,6	549466,9	426458,7	K
T04-18	13,602	12	5	132	2018	64	21,3239	17	51,5151	1288,2	0	-67,4	1220,8	555136,8	428637,2	K
T04-18	15,916	10	10	283	2018	64	21,3204	17	51,5283	1286,7	0	-67,4	1219,3	555126,2	428630,4	K
T05-18	12,625	12	5	132	2018	64	22,2666	17	43,0067	1414,5	0	-67,5	1347,1	561950,4	430519,8	K
T05-18	18,45	10	10	283	2018	64	22,2632	17	43,019	1411	0	-67,5	1343,5	561940,6	430513,3	K
T06-18	9,693	13	5	133	2018	64	24,2613	17	36,5217	1537,4	0	-67,6	1469,8	567085,9	434335,4	K
T06-18	18,24	10	10	283	2018	64	24,2575	17	36,5333	1533,7	0	-67,6	1466,1	567076,8	434328,2	K
T07-18	10,015	13	5	133	2018	64	25,2931	17	31,2059	1633,4	0	-67,7	1565,7	571312,3	436349	K
T07-18	11,737	10	10	283	2018	64	25,291	17	31,2146	1629,8	0	-67,7	1562,1	571305,4	436344,8	K
T08-18	10,55	13	5	133	2018	64	26,2953	17	27,7585	1706,8	0	-67,8	1639,1	574035,1	438276,5	K
T08-18	11,516	10	10	283	2018	64	26,295	17	27,7606	1703,6	0	-67,8	1635,9	574033,4	438275,9	K
TJsk-18	20,667	3	6	154	2018	64	2,50543	16	39,6289	1899,5	-1,55	-66,7	1831,2	614285,8	395289,1	K

Appendix D: Measured surface velocity on Vatnajökull in 2018.

Site	Calendar		Calendar		# of days	translation		velocity	
	day date	#	day date	#		(m)	(°)	(cm/day)	(m/annum)
B07-18	180509	129	181009	282	153	1,92	141	1,25	4,58
B09-18	180510	130	181009	282	152	0,78	111	0,51	1,87
B10-18	180510	130	181009	282	152	1,19	229	0,79	2,87
B11-18	180510	130	181009	282	152	7,86	21	5,17	18,88
B12-18	180510	130	181009	282	152	17,83	21	11,73	42,82
B13-18	180510	130	181009	282	152	21,40	26	14,08	51,38
B13ror15	171024	297	180509	129	197	5,68	28	2,88	10,52
B13ror15	180509	129	181009	282	153	21,68	28	14,17	51,71
B14-18	180509	129	181009	282	153	19,44	38	12,70	46,36
B15-18	180509	129	181009	282	153	12,66	48	8,27	30,20
B16-18	180509	129	181009	282	153	0,63	54	0,41	1,51
B17-18	180510	130	181009	282	152	21,40	18	14,08	51,39
B18-18	180508	128	181009	282	154	9,61	344	6,24	22,77
B19-18	180508	128	181009	282	154	0,54	306	0,35	1,27
BB0-18	180508	128	181008	281	153	0,84	253	0,55	2,00
Barc-18	180605	156	181010	283	127	3,86	99	3,04	11,08
Bor-18	180605	156	181010	283	127	4,84	154	3,81	13,92
Borth-17	171027	300	180513	133	198	19,93	195	10,07	36,74
Borth-17	180513	133	180605	156	23	2,01	200	8,72	31,83
Borth-17	180605	156	181011	284	128	1,29	247	1,01	3,68
Br2k	171029	302	180324	83	146	3,01	163	2,06	7,54
Br2-18	180324	83	180802	214	131	1,73	157	1,32	4,81
Br3-16	170328	87	180324	83	361	24,91	150	6,90	25,19
Br3-16	180324	83	180802	214	131	3,86	45	2,94	10,75
Br4-16	170328	87	180324	83	361	322,88	182	89,44	326,46
Br7-18	180509	129	181009	282	153	44,40	174	29,02	105,93
Bru-18	180508	128	181009	282	154	1,38	60	0,90	3,28
Bud-18	180508	128	181009	282	154	16,49	5	10,71	39,09
D05-18	180511	131	181010	283	152	19,13	31	12,59	45,94
D07-18	180511	131	181010	283	152	26,34	23	17,33	63,26
D09-18	180511	131	181010	283	152	6,85	348	4,50	16,44
D12-18	180511	131	181010	283	152	0,78	356	0,51	1,87
E01-18	180508	128	181009	282	154	3,34	18	2,17	7,91
E02-18	180508	128	181009	282	154	16,71	10	10,85	39,61
E03-18	180508	128	181009	282	154	8,01	343	5,20	18,98
E04-18	180508	128	181009	282	154	0,79	352	0,51	1,86
FI01-18	180508	128	181009	282	154	16,43	134	10,67	38,95
G02-18	180605	156	181010	283	127	6,76	201	5,32	19,43
G03-18	180605	156	181010	283	127	2,82	199	2,22	8,12
G04-18	180605	156	181010	283	127	0,90	9	0,71	2,59
gb2-18	180508	128	181009	282	154	12,95	354	8,41	30,69
Go1-18	180605	156	181010	283	127	2,63	162	2,07	7,56
Haab-18	180513	133	181010	283	150	0,44	303	0,29	1,07
Hof01-18	180508	128	181009	282	154	9,78	180	6,35	23,18

K01-18	180512	132	181010	283	151	4,75	287	3,14	11,48
K02-18	180512	132	181010	283	151	11,66	293	7,72	28,19
K03-18	180512	132	181010	283	151	14,46	290	9,57	34,95
K04-18	180512	132	181010	283	151	18,88	288	12,50	45,63
K05-18	180511	131	181010	283	152	11,99	245	7,89	28,80
K06-18	180605	156	181010	283	127	2,71	128	2,14	7,80
K07-18	180512	132	181010	283	151	1,19	273	0,79	2,89
S01-18	180512	132	181010	283	151	0,58	38	0,39	1,41
S02-18	180512	132	181010	283	151	15,47	190	10,24	37,39
S04-18	180512	132	181010	283	151	21,18	205	14,02	51,19
S05-18	180512	132	181010	283	151	11,23	254	7,44	27,14
Ske02-18	180513	133	181009	282	149	30,15	223	20,24	73,86
Ske04-18	180509	129	181009	282	153	46,83	228	30,61	111,73
Ske05-18	180509	129	181009	282	153	21,57	209	14,10	51,46
Skf00-18	180507	127	181008	281	154	2,81	46	1,82	6,66
Skf01-18	180508	128	181008	281	153	11,77	110	7,70	28,09
T01ve-18	180512	132	181010	283	151	1,20	162	0,80	2,91
T02-18	180512	132	181010	283	151	3,87	278	2,56	9,35
T03-18	180512	132	181010	283	151	7,66	247	5,07	18,51
T04-18	180512	132	181010	283	151	12,52	238	8,29	30,27
T05-18	180512	132	181010	283	151	11,69	238	7,74	28,25
T06-18	180513	133	181010	283	150	11,66	233	7,77	28,37
T07-18	180513	133	181010	283	150	8,06	240	5,38	19,62
T08-18	180513	133	181010	283	150	1,82	251	1,21	4,42

Appendix E: Melt water runoff to selected rivers in summer 2018, derived from summer surface balance.

ΔS : area in a given elevation range where summer balance is negative, $\Sigma\Delta S$: cumulative area above a given elevation, ΔQ_s : melt water runoff from a given elevation range, $\Sigma\Delta Q_s$: cumulative melt water runoff from an area above given elevation.

Tungnaá water drainage basin

Elevation (m a. s. l.)		ΔS km^2	$\Sigma\Delta S$ km^2	ΔQ_s (10^6m^3)	$\Sigma\Delta Q_s$ (10^6m^3)
1350	1400	0,4	0,4	0,4	0,4
1300	1350	6,1	6,4	6,9	7,3
1250	1300	10,2	16,7	13,3	20,6
1200	1250	10,9	27,6	16,2	36,8
1150	1200	9,9	37,5	16,9	53,7
1100	1150	11,9	49,4	23,0	76,7
1050	1100	11,9	61,4	26,4	103,1
1000	1050	9,6	71,0	23,9	127,0
950	1000	9,6	80,6	26,7	153,7
900	950	9,2	89,8	29,2	182,9
850	900	7,8	97,5	28,7	211,7
800	850	7,7	105,2	33,0	244,6
750	800	7,0	112,1	33,7	278,3
700	750	4,7	116,9	24,5	302,8
650	700	2,1	119,0	11,3	314,1

Sylgja water drainage basin

Elevation (m a. s. l.)		ΔS km^2	$\Sigma\Delta S$ km^2	ΔQ_s (10^6m^3)	$\Sigma\Delta Q_s$ (10^6m^3)
1300	1350	1,1	1,1	1,3	1,3
1250	1300	3,6	4,7	4,6	5,9
1200	1250	5,9	10,5	8,7	14,6
1150	1200	8,3	18,8	13,7	28,4
1100	1150	6,1	24,9	11,2	39,5
1050	1100	6,9	31,8	14,6	54,1
1000	1050	5,1	36,9	13,2	67,3
950	1000	1,8	38,7	4,7	72,1
900	950	0,7	39,3	1,9	74,0
850	900	0,0	39,4	0,2	74,2

Western Skaftá cauldron water drainage basin

Elevation (m a. s. l.)		ΔS km^2	$\Sigma\Delta S$ km^2	ΔQ_s (10^6m^3)	$\Sigma\Delta Q_s$ (10^6m^3)
1700	1750	2,5	2,5	0,7	0,7
1650	1700	7,2	9,7	2,3	3,0
1600	1650	8,5	18,2	3,2	6,1
1550	1600	5,4	23,6	2,3	8,5
1500	1550	1,5	25,1	0,7	9,2

Eastern Skaftár cauldron water drainage basin

Elevation (m a. s. l.)		ΔS km ²	$\Sigma \Delta S$ km ²	ΔQ_s (10 ⁶ m ³)	$\Sigma \Delta Q_s$ (10 ⁶ m ³)
1750	1800	2,4	2,4	0,4	0,4
1700	1750	9,9	12,3	3,2	3,7
1650	1700	14,9	27,2	6,5	10,2
1600	1650	9,7	36,9	3,9	14,1
1550	1600	2,4	39,3	1,0	15,0

Grímsvötn water drainage basin

Elevation (m a. s. l.)		ΔS km ²	$\Sigma \Delta S$ km ²	ΔQ_s (10 ⁶ m ³)	$\Sigma \Delta Q_s$ (10 ⁶ m ³)
1800	1850	0,3	0,3	0,0	0,0
1750	1800	4,3	4,6	0,9	0,9
1700	1750	18,6	23,2	7,2	8,1
1650	1700	53,3	76,4	25,5	33,6
1600	1650	30,9	107,3	19,9	53,6
1550	1600	19,3	126,5	16,7	70,3
1500	1550	16,8	143,3	18,9	89,2
1450	1500	10,0	153,3	12,8	102,0
1400	1450	11,7	165,0	15,7	117,8
1350	1400	4,3	169,4	5,9	123,6
1300	1350	0,7	170,1	1,0	124,6

Kaldakvísl water drainage basin

Elevation (m a. s. l.)		ΔS km ²	$\Sigma \Delta S$ km ²	ΔQ_s (10 ⁶ m ³)	$\Sigma \Delta Q_s$ (10 ⁶ m ³)
1850	1900	0,2	0,2	0,0	0,0
1800	1850	0,7	0,8	0,0	0,0
1750	1800	9,3	10,2	0,6	0,6
1700	1750	20,2	30,4	3,3	3,9
1650	1700	17,1	47,4	4,6	8,6
1600	1650	14,5	61,9	5,7	14,3
1550	1600	19,1	81,0	10,3	24,6
1500	1550	25,3	106,3	17,7	42,3
1450	1500	28,8	135,1	23,0	65,3
1400	1450	24,0	159,1	21,9	87,2
1350	1400	22,1	181,2	24,1	111,3
1300	1350	21,2	202,4	28,0	139,3
1250	1300	22,4	224,8	34,5	173,8
1200	1250	21,7	246,5	38,0	211,8
1150	1200	20,0	266,5	41,5	253,3
1100	1150	18,0	284,4	46,7	300,0
1050	1100	16,9	301,3	52,6	352,6
1000	1050	14,6	315,9	53,1	405,6
950	1000	10,4	326,3	43,0	448,6
900	950	6,3	332,7	27,4	476,0
850	900	0,9	333,5	3,9	479,9

Jökulsá á Fjöllum water drainage basin

Elevation (m a. s. l.)		ΔS km ²	$\Sigma \Delta S$ km ²	ΔQ_s (10 ⁶ m ³)	$\Sigma \Delta Q_s$ (10 ⁶ m ³)
1900	1950	0,0	0,0	0,0	0,0
1850	1900	0,6	0,7	0,0	0,0
1800	1850	3,4	4,1	0,0	0,0
1750	1800	20,9	25,0	1,9	2,0
1700	1750	34,4	59,4	6,3	8,3
1650	1700	80,7	140,1	25,0	33,3
1600	1650	121,1	261,2	44,6	77,9
1550	1600	100,5	361,7	44,0	121,9
1500	1550	93,6	455,3	51,7	173,6
1450	1500	80,6	535,9	55,7	229,3
1400	1450	69,8	605,7	59,6	289,0
1350	1400	56,3	662,0	60,1	349,1
1300	1350	43,3	705,3	57,0	406,1
1250	1300	47,2	752,5	75,9	482,1
1200	1250	51,6	804,1	103,0	585,1
1150	1200	51,4	855,5	128,8	713,8
1100	1150	44,8	900,3	133,8	847,6
1050	1100	32,3	932,6	109,7	957,3
1000	1050	33,5	966,1	125,6	1082,9
950	1000	31,0	997,0	129,3	1212,2
900	950	26,0	1023,1	120,9	1333,1
850	900	23,7	1046,8	120,4	1453,6
800	850	21,6	1068,4	117,1	1570,7
750	800	17,8	1086,1	102,9	1673,6
700	750	5,4	1091,5	32,6	1706,2

Kreppa and Kverká water drainage basin

Elevation (m a. s. l.)		ΔS km ²	$\Sigma \Delta S$ km ²	ΔQ_s (10 ⁶ m ³)	$\Sigma \Delta Q_s$ (10 ⁶ m ³)
1850	1900	0,9	1,0	0,0	0,1
1800	1850	0,6	1,6	0,0	0,1
1750	1800	2,2	3,8	0,2	0,3
1700	1750	3,8	7,6	0,6	0,9
1650	1700	5,2	12,8	1,4	2,3
1600	1650	41,4	54,2	18,8	21,1
1550	1600	20,5	74,7	11,3	32,4
1500	1550	13,4	88,1	8,2	40,6
1450	1500	16,3	104,4	10,8	51,4
1400	1450	19,8	124,2	14,4	65,8
1350	1400	25,5	149,6	21,8	87,6
1300	1350	20,0	169,7	20,7	108,3
1250	1300	15,5	185,2	18,4	126,7
1200	1250	17,7	202,9	23,5	150,2
1150	1200	17,7	220,6	26,8	176,9
1100	1150	16,9	237,5	31,1	208,0
1050	1100	11,1	248,6	31,3	239,3
1000	1050	13,4	262,0	30,8	270,1
950	1000	15,1	277,1	49,1	319,2
900	950	13,5	290,6	59,1	378,3
850	900	14,2	304,8	65,3	443,6
800	850	11,0	315,8	58,9	502,5
750	800	10,5	326,3	59,9	562,4
700	750	4,8	331,1	28,9	591,3
650	700	1,8	332,9	9,5	600,8

Háslón water drainage basin

Elevation (m a. s. l.)		ΔS km ²	$\Sigma \Delta S$ km ²	ΔQ_s (10 ⁶ m ³)	$\Sigma \Delta Q_s$ (10 ⁶ m ³)
1600	1650	11,2	11,2	5,3	5,3
1550	1600	31,8	43,0	15,5	20,8
1500	1550	63,6	106,7	32,6	53,4
1450	1500	67,6	174,3	37,3	90,7
1400	1450	97,7	272,0	63,9	154,6
1350	1400	131,7	403,7	110,7	265,3
1300	1350	129,4	533,1	125,4	390,7
1250	1300	126,1	659,2	131,6	522,3
1200	1250	99,2	758,4	111,4	633,7
1150	1200	84,7	843,1	112,3	745,9
1100	1150	66,5	909,6	118,6	864,6
1050	1100	58,7	968,3	141,4	1006,0
1000	1050	49,4	1017,7	145,4	1151,4
950	1000	41,4	1059,2	142,5	1293,9
900	950	32,9	1092,0	128,9	1422,8
850	900	28,5	1120,5	124,2	1547,0
800	850	27,2	1147,7	128,7	1675,6
750	800	26,6	1174,3	135,3	1810,9
700	750	20,8	1195,1	112,6	1923,6
650	700	15,7	1210,7	89,9	2013,5
600	650	3,0	1213,7	18,1	2031,6

Jökulsá á Fljótsdal water drainage basin

Elevation (m a. s. l.)		ΔS km^2	$\Sigma \Delta S$ km^2	ΔQ_s (10^6m^3)	$\Sigma \Delta Q_s$ (10^6m^3)
1450	1500	0,9	1,0	0,9	1,0
1400	1450	1,9	2,9	1,9	2,9
1350	1400	2,8	5,8	3,0	5,9
1300	1350	5,4	11,2	6,0	11,9
1250	1300	16,2	27,4	16,8	28,7
1200	1250	16,0	43,4	20,1	48,8
1150	1200	17,3	60,7	26,2	75,1
1100	1150	15,0	75,7	28,6	103,7
1050	1100	12,4	88,1	31,1	134,7
1000	1050	11,9	100,0	35,8	170,5
950	1000	8,8	108,8	30,7	201,2
900	950	5,5	114,3	21,8	223,0
850	900	4,4	118,7	18,6	241,6
800	850	3,2	121,9	14,7	256,3
750	800	3,0	124,9	15,5	271,7
700	750	2,6	127,5	14,7	286,4
650	700	3,0	130,6	18,3	304,7
600	650	0,2	130,7	1,0	305,7

Hornafjarðarfljót water drainage basin

Elevation (m a. s. l.)		ΔS km ²	$\Sigma \Delta S$ km ²	ΔQ_s (10 ⁶ m ³)	$\Sigma \Delta Q_s$ (10 ⁶ m ³)
1450	1500	1,0	1,0	1,0	1,0
1400	1450	8,2	9,2	7,3	8,3
1350	1400	12,7	21,8	12,1	20,4
1300	1350	19,1	40,9	20,2	40,6
1250	1300	37,9	78,9	39,7	80,2
1200	1250	29,1	108,0	34,1	114,3
1150	1200	20,5	128,4	27,3	141,6
1100	1150	19,1	147,5	28,4	170,0
1050	1100	14,5	162,0	24,3	194,3
1000	1050	11,4	173,4	21,3	215,5
950	1000	10,7	184,2	21,5	237,1
900	950	8,2	192,3	17,5	254,6
850	900	5,5	197,8	12,6	267,2
800	850	4,4	202,2	10,5	277,7
750	800	4,2	206,3	10,4	288,1
700	750	3,7	210,1	9,7	297,8
650	700	3,6	213,6	9,6	307,5
600	650	2,6	216,3	7,5	315,0
550	600	1,9	218,2	5,7	320,6
500	550	1,9	220,1	6,0	326,6
450	500	1,3	221,4	4,4	331,0
400	450	1,3	222,7	5,0	336,0
350	400	0,8	223,6	3,6	339,6
300	350	0,9	224,5	4,2	343,8
250	300	1,5	225,9	7,6	351,4
200	250	2,9	228,8	16,3	367,7
150	200	3,1	232,0	19,7	387,4
100	150	2,4	234,4	16,1	403,5
50	100	1,8	236,2	12,8	416,2
0	50	2,6	238,9	19,1	435,4

Jökulsá á Breiðamerkursandi water drainage basin

Elevation (m a. s. l.)		ΔS km ²	$\Sigma \Delta S$ km ²	ΔQ_s (10 ⁶ m ³)	$\Sigma \Delta Q_s$ (10 ⁶ m ³)
1700	1750	0,5	0,5	0,0	0,0
1650	1700	4,2	4,7	0,6	0,6
1600	1650	13,8	18,5	4,5	5,1
1550	1600	19,0	37,5	7,7	12,8
1500	1550	23,2	60,7	11,3	24,1
1450	1500	36,2	96,9	21,8	45,9
1400	1450	51,2	148,1	38,7	84,6
1350	1400	84,2	232,3	82,5	167,2
1300	1350	83,4	315,8	95,2	262,4
1250	1300	51,6	367,4	65,9	328,3
1200	1250	35,1	402,5	48,4	376,7
1150	1200	28,2	430,7	41,8	418,6
1100	1150	24,1	454,8	38,5	457,1
1050	1100	20,5	475,2	35,1	492,2
1000	1050	17,6	492,8	32,2	524,4
950	1000	18,9	511,8	36,1	560,5
900	950	20,0	531,8	39,7	600,3
850	900	19,9	551,7	43,1	643,4
800	850	20,1	571,9	47,6	690,9
750	800	19,5	591,4	51,4	742,3
700	750	19,2	610,6	54,8	797,1
650	700	27,6	638,2	82,8	879,9
600	650	18,4	656,6	59,9	939,8
550	600	18,7	675,3	66,5	1006,3
500	550	7,6	682,9	27,0	1033,3
450	500	6,5	689,3	24,9	1058,2
400	450	6,4	695,7	25,1	1083,3
350	400	5,3	700,9	22,2	1105,4
300	350	5,7	706,6	26,7	1132,1
250	300	5,5	712,1	28,5	1160,7
200	250	5,9	718,0	33,7	1194,3
150	200	5,3	723,3	33,6	1227,9
100	150	4,9	728,2	33,5	1261,4
50	100	4,8	733,1	34,5	1295,9
0	50	3,9	736,9	28,5	1324,5

Breiðárlón/Fjallsárlón water drainage basin

Elevation (m a. s. l.)		ΔS km ²	$\Sigma \Delta S$ km ²	ΔQ_s (10 ⁶ m ³)	$\Sigma \Delta Q_s$ (10 ⁶ m ³)
1800	1850	0,1	0,1	0,0	0,0
1750	1800	2,1	2,2	0,1	0,1
1700	1750	2,9	5,2	0,5	0,6
1650	1700	3,0	8,1	0,8	1,5
1600	1650	4,2	12,4	1,7	3,2
1550	1600	4,3	16,7	2,4	5,6
1500	1550	5,7	22,4	3,9	9,5
1450	1500	4,9	27,3	3,9	13,4
1400	1450	5,3	32,7	4,9	18,3
1350	1400	6,3	39,0	6,6	25,0
1300	1350	12,6	51,6	15,2	40,2
1250	1300	6,5	58,1	8,2	48,3
1200	1250	5,6	63,7	7,5	55,8
1150	1200	4,9	68,5	6,9	62,7
1100	1150	4,5	73,0	7,0	69,7
1050	1100	5,0	78,0	8,3	78,0
1000	1050	6,0	83,9	10,5	88,5
950	1000	6,9	90,8	13,2	101,7
900	950	8,3	99,1	16,8	118,5
850	900	6,6	105,7	14,6	133,1
800	850	8,1	113,8	19,4	152,5
750	800	8,7	122,5	23,3	175,8
700	750	6,2	128,8	18,0	193,8
650	700	7,1	135,8	21,9	215,7
600	650	7,9	143,7	26,0	241,7
550	600	8,6	152,3	30,5	272,1
500	550	8,7	161,0	31,5	303,7
450	500	9,1	170,0	34,3	338,0
400	450	11,0	181,0	43,4	381,5
350	400	8,9	189,9	37,7	419,2
300	350	6,9	196,8	31,8	451,0
250	300	6,9	203,7	35,6	486,6
200	250	7,1	210,8	40,4	527,0
150	200	5,3	216,1	33,2	560,2
100	150	4,3	220,4	29,0	589,1
50	100	4,1	224,5	28,4	617,5
0	50	3,3	227,8	23,8	641,3

Skeiðarársandur (Gígja) water drainage basin (Gígja)

Elevation (m a. s. l.)		ΔS km^2	$\Sigma \Delta S$ km^2	ΔQ_s (10^6m^3)	$\Sigma \Delta Q_s$ (10^6m^3)
1700	1750	0,6	0,6	0,0	0,0
1650	1700	18,3	18,9	7,0	7,0
1600	1650	80,9	99,8	35,5	42,5
1550	1600	82,0	181,8	40,9	83,4
1500	1550	105,5	287,3	61,2	144,6
1450	1500	96,3	383,6	73,7	218,3
1400	1450	92,7	476,3	95,7	314,1
1350	1400	81,5	557,8	108,2	422,3
1300	1350	69,9	627,7	102,5	524,9
1250	1300	62,9	690,6	98,9	623,8
1200	1250	52,5	743,2	88,3	712,1
1150	1200	44,8	787,9	82,3	794,4
1100	1150	37,2	825,2	75,3	869,6
1050	1100	30,5	855,7	67,9	937,5
1000	1050	24,6	880,3	59,2	996,7
950	1000	23,1	903,3	59,5	1056,2
900	950	23,4	926,7	64,0	1120,2
850	900	28,4	955,1	82,8	1203,0
800	850	21,2	976,4	66,0	1269,0
750	800	18,6	995,0	61,5	1330,5
700	750	20,1	1015,1	69,5	1400,1
650	700	14,2	1029,2	51,7	1451,8
600	650	11,6	1040,8	43,6	1495,4
550	600	13,9	1054,7	55,2	1550,6
500	550	9,4	1064,0	39,3	1589,9
450	500	6,3	1070,3	27,7	1617,5
400	450	6,6	1076,9	30,5	1648,1
350	400	9,2	1086,1	45,4	1693,4
300	350	12,3	1098,4	64,8	1758,2
250	300	12,7	1111,1	70,9	1829,1
200	250	12,6	1123,7	73,9	1903,0
150	200	10,5	1134,2	64,8	1967,8
100	150	8,9	1143,1	56,9	2024,7
50	100	7,9	1151,1	52,3	2077,0
0	50	0,2	1151,2	1,1	2078,1

Súla water drainage basin

Elevation (m a. s. l.)		ΔS km ²	$\Sigma \Delta S$ km ²	ΔQ_s (10 ⁶ m ³)	$\Sigma \Delta Q_s$ (10 ⁶ m ³)
1700	1750	0,5	0,5	0,0	0,0
1650	1700	1,5	1,9	0,3	0,4
1600	1650	2,5	4,4	1,0	1,3
1550	1600	4,0	8,5	2,0	3,3
1500	1550	5,9	14,3	3,5	6,8
1450	1500	11,1	25,4	7,9	14,8
1400	1450	11,0	36,4	9,4	24,2
1350	1400	9,3	45,7	9,8	34,0
1300	1350	8,2	53,9	9,8	43,8
1250	1300	6,6	60,5	8,8	52,7
1200	1250	7,9	68,4	11,8	64,5
1150	1200	8,8	77,2	15,0	79,5
1100	1150	15,2	92,4	28,6	108,1
1050	1100	16,0	108,3	34,0	142,1
1000	1050	16,7	125,0	39,7	181,8
950	1000	18,0	143,0	47,3	229,1
900	950	15,4	158,4	43,8	272,9
850	900	11,4	169,7	33,9	306,8
800	850	11,9	181,6	37,0	343,8
750	800	7,4	189,0	24,8	368,6
700	750	5,9	194,9	21,5	390,2
650	700	5,1	200,0	19,0	409,2
600	650	5,6	205,6	21,5	430,7
550	600	11,1	216,7	43,4	474,1
500	550	10,5	227,2	42,4	516,5
450	500	7,3	234,5	31,3	547,8
400	450	6,5	241,0	29,6	577,4
350	400	5,1	246,0	24,8	602,2
300	350	2,7	248,7	14,3	616,5
250	300	1,0	249,7	5,9	622,4
200	250	0,8	250,6	4,9	627,3
150	200	0,7	251,3	4,2	631,5
100	150	0,7	252,0	4,6	636,1
50	100	0,7	252,7	5,1	641,1

Djúpá water drainage basin

Elevation (m a. s. l.)		ΔS km^2	$\Sigma \Delta S$ km^2	ΔQ_s (10^6m^3)	$\Sigma \Delta Q_s$ (10^6m^3)
1450	1500	0,0	0,0	0,0	0,0
1400	1450	0,3	0,4	0,3	0,4
1350	1400	0,7	1,1	0,8	1,2
1300	1350	3,5	4,6	3,8	5,0
1250	1300	3,4	8,0	3,9	8,9
1200	1250	3,0	11,0	3,9	12,7
1150	1200	3,5	14,5	5,4	18,1
1100	1150	5,3	19,9	9,3	27,4
1050	1100	6,1	26,0	12,6	40,1
1000	1050	9,2	35,2	21,9	61,9
950	1000	7,3	42,4	20,2	82,2
900	950	7,8	50,2	23,7	105,9
850	900	6,7	56,9	21,7	127,6
800	850	8,0	64,8	27,7	155,2
750	800	6,6	71,4	23,9	179,1
700	750	3,7	75,1	14,1	193,2
650	700	2,9	78,0	11,6	204,9
600	650	1,0	79,0	4,2	209,0

Brunná water drainage basin

Elevation (m a. s. l.)		ΔS km^2	$\Sigma \Delta S$ km^2	ΔQ_s (10^6m^3)	$\Sigma \Delta Q_s$ (10^6m^3)
1050	1100	0,0	0,0	0,0	0,0
1000	1050	0,9	1,0	2,3	2,3
950	1000	2,5	3,5	6,8	9,1
900	950	4,3	7,8	13,2	22,3
850	900	4,2	12,0	13,8	36,2
800	850	4,2	16,2	14,3	50,4
750	800	4,6	20,7	16,3	66,8
700	750	5,6	26,4	21,2	88,0
650	700	4,8	31,2	19,3	107,3
600	650	3,2	34,4	13,3	120,6
550	600	0,5	34,9	2,2	122,8

Hverfisfljót water drainage basin

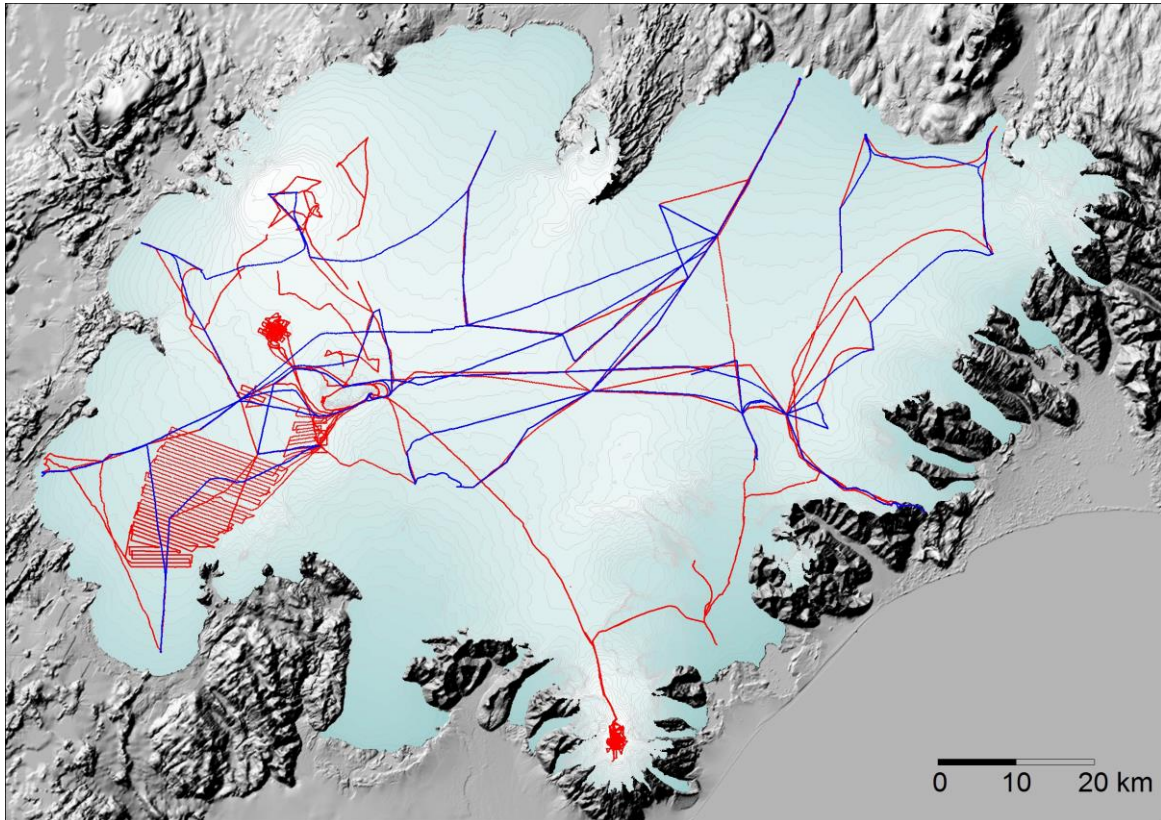
Elevation (m a. s. l.)		ΔS km ²	$\Sigma \Delta S$ km ²	ΔQ_s (10 ⁶ m ³)	$\Sigma \Delta Q_s$ (10 ⁶ m ³)
1700	1750	0,5	0,5	0,0	0,0
1650	1700	5,5	6,0	1,6	1,6
1600	1650	9,1	15,0	3,5	5,1
1550	1600	9,6	24,7	4,0	9,1
1500	1550	19,9	44,6	9,7	18,8
1450	1500	41,1	85,6	27,9	46,7
1400	1450	27,6	113,2	23,0	69,7
1350	1400	24,1	137,4	23,9	93,6
1300	1350	22,8	160,2	25,4	119,0
1250	1300	18,1	178,3	22,3	141,3
1200	1250	20,2	198,5	26,9	168,1
1150	1200	14,6	213,1	21,9	190,0
1100	1150	11,1	224,1	19,7	209,7
1050	1100	9,6	233,7	19,5	229,2
1000	1050	9,0	242,7	21,3	250,5
950	1000	8,9	251,6	24,0	274,5
900	950	8,6	260,1	26,0	300,4
850	900	7,8	267,9	25,4	325,8
800	850	7,3	275,1	25,0	350,8
750	800	10,1	285,2	36,4	387,2
700	750	12,1	297,3	46,4	433,6
650	700	10,5	307,8	42,7	476,3
600	650	6,2	314,0	26,0	502,3
550	600	1,0	315,0	4,4	506,7

Skaftá water drainage basin

Elevation (m a. s. l.)		ΔS km ²	$\Sigma \Delta S$ km ²	ΔQ_s (10 ⁶ m ³)	$\Sigma \Delta Q_s$ (10 ⁶ m ³)
1650	1700	2,2	2,2	1,0	1,0
1600	1650	15,6	17,8	6,4	7,4
1550	1600	22,7	40,4	9,9	17,3
1500	1550	30,8	71,2	17,2	34,5
1450	1500	24,5	95,7	16,2	50,7
1400	1450	22,3	118,0	18,3	69,1
1350	1400	20,5	138,5	20,3	89,3
1300	1350	22,5	161,0	25,6	115,0
1250	1300	15,6	176,6	19,9	134,8
1200	1250	21,0	197,6	30,0	164,9
1150	1200	22,7	220,2	36,9	201,8
1100	1150	23,7	243,9	44,6	246,4
1050	1100	24,2	268,1	52,9	299,3
1000	1050	26,2	294,3	65,5	364,8
950	1000	20,6	314,9	58,8	423,6
900	950	16,7	331,7	53,3	476,9
850	900	14,4	346,0	50,8	527,7
800	850	14,8	360,8	58,4	586,1
750	800	12,3	373,1	53,9	640,0
700	750	9,7	382,8	45,5	685,5
650	700	5,8	388,6	28,3	713,8
600	650	1,1	389,7	5,6	719,4

Appendix F: location of GPS surface profiles 2018.

During field trips, GPS L1, L2 land survey instruments mounted on snow tracks, cars or snowmobiles are used to collect data continuously. The collected data is kinematically postprocessed, usually with accuracy of a few centimeters for position of the antenna center, and surface elevation with an accuracy of few cm to few dm, depending on stability of the vehicle.



Location of GPS surface profiles 2018. Profiles surveyed in March, May and June shown in RED and surveyed in October in BLUE.